

Responses to the Comments of Referee #1

(1) The objectives set out for the work in the last paragraph in the introduction are rather unambitious and relate to the effect of the Paris megacity on the downwind areas, and the frequency and spatial characteristics of new particle formation events. To address such objectives fully would require measurements over at least a full year but these were in fact limited to campaigns of one month in summer and one in winter, and these are not set in the context of a long-term dataset so it is not known whether they are representative or not.

A complete year of size distribution measurements (including the two intensive campaigns discussed in the present paper) has been recently presented by Dos Santos et al. (2015). These measurements took place in one site in the center of Paris (LHVP station) from July 2009 to September 2010. During this year, the highest NPF frequency in Paris was observed during July 2009 (the summer campaign examined in this work) and the lowest during the winter (which includes the winter campaign in this work). Therefore this work focuses on two extreme NPF periods in Paris. During summer under clean conditions and peak NPF frequency and during winter under polluted conditions and minimal NPF frequency. These are now explained in the revised manuscript, placing the work in the context of a longer-term dataset as the reviewer suggested.

(2) The title refers to ultrafine particle sources but the reader learns only about NPF events and nothing about the other sources of particles. Either the title needs to change or the content needs to be enhanced if possible to throw light on other sources, although the design of the experiments is not good from this perspective.

We do agree with the point of the reviewer. The title of the paper has been changed to “In situ formation and spatial variability of particle number concentration in a European Megacity”, which better describes the final scope of this paper.

(3) From the section on instrumentation and the list of instruments in Table 1, it is clear that ultrafine particle measurements were made with a substantial range of different instruments using at least two different methods of drying of the air stream. For some of the instruments, the drying method is not clear and it would be useful if these were added to Table 1. Given the substantial range of instruments and at least two drying methods, it would be essential to intercompare the CPCs with one another and the SMPS/DMPS/EAS instruments with one another. This is not reported and there are consequently question marks over the comparability of measurements by the different instruments. If an intercomparison was conducted, this needs to be included and a description given of how divergences in readings were accommodated in the data analysis.

The sampling conditions (dry/ambient) are now explicitly stated in Table 1. The different instruments were intercompared during both campaigns. At least one of the mobile laboratories visited each site for several hours (5-15 h) during each campaign. The summary of these comparisons is shown in a new figure in the supplementary material (Fig. S1). During summer, the differences in number concentration between the CPC on board the visiting mobile laboratory (MOSQUITA) and the aerosol sizing instrument at each of the stationary sites did not exceed 10%. During winter the discrepancies were higher mainly due to the lower detection efficiency size limit of the MoLa CPC that was used for the intercomparisons. During both campaigns the number concentrations monitored onboard MoLa and MOSQUITA were also

compared for approximately 8 hours. The two instruments were found to agree during periods without nucleation. The comparison of the CPCs in the two mobile laboratories has been presented by von der Weiden-Reinmüller et al. (2014). A brief summary of the intercomparisons together with the corresponding references to previous work have been added in the revised paper.

(4) It has been noted by a number of authors that both particle number counts and particle size distributions in urban areas changed substantially with the introduction of zero sulphur motor fuels. This effect needs to be mentioned together with information on the sulphur content of motor fuels in the Paris region at the time of these experiments. This critically affects the particle size distribution and aerosol lifetime. Most (61%) of light duty vehicles in France during the period of the measurements were using diesel fuel with 10 ppm sulfur. As the reviewer has indicated both the sulfur content and the fuel type dictate vehicle emissions. This is now discussed in the revised manuscript.

(5) Section 3.1 deals with the estimation of condensation sinks, but the method by which these were estimated is not adequately described. Section 3.3 gives adequate detail on how the humidity-adjusted size distribution was calculated but this is only part of the method

A detailed description of the condensation sink estimation, including the corresponding equations, is presented in the revised manuscript.

(6) Figure 8 shows average size distributions for each season and site and these are briefly discussed on page 5676 going into 5677. Given that the paper, judging from the title, is concerned with the sources of ultrafine particles and that other workers have sought to elicit source information from number size distributions, this section is very disappointing and gives few if any insights into the factors giving rise to these size distributions. The quite substantial differences between summer and winter are not explained other than by an indication that similar behaviour has been observed elsewhere, and the inter-site differences are described but not explained.

The discussion based upon the size distributions has been expanded focusing on the sizes of the various modes and their strength. As mentioned above, the title of the paper has been changed to avoid confusion about its focus on the primary and secondary particle number sources and not on the individual primary sources.

(7) The discussion of new particle formation in Section 6 is one of the stronger parts of the paper but the critical omission is the measurement of sulphur dioxide concentrations. Are there no useful data available from anywhere within the domain of the experiments? Without this information, the discussion is very incomplete as the authors acknowledge at the end of page 5685.

Sulfur dioxide measurements were available at GOLF which was mostly downwind of Paris during the summer campaign. However, the low sulfur content of vehicle emissions and the lack of other major sulfur sources resulted in ambient sulfur dioxide concentrations that were below the detection limit (0.5 ppb) of the instrument used most of the time. As a result, there is little useful information in these measurements. This is now mentioned in the revised paper.

(8) Page 6598, line 1 – the spelling of authors' names is incorrect.

We checked the spelling of the authors' names in the Wang et al. (2010) reference in page 5698 and it is correct.

(9) Page 5710, legend to Figure 10, 3rd line – should read exponential decrease (not decease).

Corrected

References

Dos Santos, V. N., Herrmann, E., Manninen, H. E., Hussein, T., Hakala, J., Nieminen, T., Aalto, P. P., Merkel, M., Wiedensohler, A., Kulmala, M., Petäjä, T., and Hämeri, K.: Variability of air ion concentrations in urban Paris, *Atmos. Chem. Phys. Discuss.*, 15, 10629-10676, doi:10.5194/acpd-15-10629-2015, 2015.

von der Weiden-Reinmüller, S.-L., Drewnick, F., Crippa, M., Prévôt, A. S. H., Meleux, F., Baltensperger, U., Beekmann, M., and Borrmann, S.: Application of mobile aerosol and trace gas measurements for the investigation of megacity air pollution emissions: the Paris metropolitan area, *Atmos. Meas. Tech.*, 7, 279-299, 2014a.

Response to the Comments of Referee #2

(1) The paper was an enjoyable read to start with, and well written. However it became evident that the sources of the NPF events were not going to be identified, as the paper title suggested.

We do agree with the point of the reviewer. The title of the paper has been changed to “In situ formation and spatial variability of particle number concentration in a European Megacity”, which better describes the final scope of this paper. The scope and analysis of this work have not changed. These include

- analysis of NPF events within, downwind and upwind of Paris that suggest that the condensational sink was the dominant factor influencing the frequency of events in this Megacity.

- effect of the Paris emissions on particle number concentrations around the Megacity.

(2) The Paris plume itself was identified by concentrations of black carbon and increased particle numbers. I wonder whether non-Paris contributions of black carbon might affect this assumption – i.e. smoke from rural grass/forest fires in summer, or suburban/rural wood burning in winter?

We have examined satellite-based products for fire identification, including small fires. No biomass burning events, significant enough to be identified by the algorithm used (Randerson et al., 2012), were observed during the two campaigns. Thus during summer biomass burning was ruled out as a potential source of error. On the other hand, during winter areas outside of the Paris plume with increased black carbon levels were identified and omitted from the analysis. The black carbon source in these cases was residential biomass burning. The particle number concentrations in these areas were relatively low though. The potential interference of these sources would have a modest to small effect on our estimates regarding the evolution of the Paris aerosol number plume. A new paragraph has been added in the revised manuscript discussing the above point.

(3) The paper explained when new particle formation takes place and whether agreeable measurements were made at other sites but does not explain the process of formation nor what the particles are composed of. I would expect that an experiment designed to investigate ultrafine particle sources would have had an aerosol speciation instrument, such as an Aerosol Mass Spectrometer or an Aerosol Chemical Speciation Monitor available.

The MEGAPOLI measurements focused on the identification of particulate matter mass sources. There were three AMS units available in the three sites and a detailed analysis of their measurements can be found in the corresponding publications (Freutel et al., 2013; Crippa et al., 2013a; 2013b; 2013c). A synthesis of all the fine PM source attribution measurements has been provided by Beekmann et al. (2015). Unfortunately, all these refer to the fine PM (PM_1 and $PM_{2.5}$) mass concentration and not to the new particles. The mass of the new particles is a very small fraction of the total and the corresponding compositions can be very different. The new particle formation events took place during periods with relative rapid photochemistry so all secondary particle components increased at the same time. We have added some text in the revised paper discussing the above points.

(4) From the list of instrumentation used in Table 1, the only coincident trace gas measurements were taken on board the aircraft at approx 600 m in height. None of

these trace gases correlated with particle number. Why were there no ground measurements of trace gases? A brief look at papers within the MEGAPOLI special issue suggests there are more measurements available, indeed the section describing the MEGAPOLI field campaign in the introduction discusses other work done to identify sources of particulate matter, but then these same measurements don't seem to be used later on to help identify the sources of these ultrafine particles.

Table 1 presents a subset of the MEGAPOLI measurements that have been used in this work. There were several additional gas-phase measurements in the ground stations (see for example Michoud et al., 2012). These measurements (OH, ROx, NO, NO₂, O₃, CO, PAN, HONO, VOCs) did not provide any additional insights about the precursors of new particles formed. We have added in the text references to the papers providing detailed information about the gas-phase measurements that took place during the MEGAPOLI campaigns.

(5) Was any modeling done across the MEGAPOLI participants to try and answer these questions? The CHIMERE model is mentioned in the introduction section as being used to decide the routes of the mobile and aircraft platforms, but could have been used to model the Paris Plume. This would then have pointed to certain emission source groups being likely candidates for the different NPF events. Even better, a model incorporating aerosol number, size and composition would aid the story.

There have been a number of modeling efforts but all of them have focused so far on particle mass and not number. The Zhang et al. (2013) study using CHIMERE and the Couvidat et al. (2013) work investigated the sources of organic aerosol in Paris. Skyllakou et al. (2014) examined the contributions of local and regional sources to fine PM mass concentrations in Paris. However, sources that contribute significantly to particle mass may contribute little to particle number or vice versa depending on the corresponding size distributions. Extrapolating from the particle mass source attribution studies to particle number is dangerous. There have been no modeling studies yet focusing on both aerosol number and mass. We do agree with the reviewer that such studies together with the MEGAPOLI measurements could provide valuable insights. References to the MEGAPOLI modeling studies have been added to the revised paper.

(6) Please explain the comment “during winter the higher condensation sink...prevented particles from growing to sizes larger than 10 nm”. I would expect that high condensation would lead to an increase in the particle size either directly or via coagulation. The only other explanation is that there was a high surface area already present which caused a plateau in the particle growth, but as there were no nucleation events in winter I don't understand where this high surface area originated from.

The reviewer is correct; there was a high surface area already present resulting in the high condensation sink. The sources of these particles included long range transport, biomass burning, transportation, cooking, etc. (Crippa et al., 2013a). These sources provided plenty of aerosol surface area. This is now explained in Section 5.1 of the revised manuscript.

References

Beekmann, M., Prévôt, A. S. H., Drewnick, F., Sciare, J., Pandis, S. N., Denier van der Gon, H. A. C., Crippa, M., Freutel, F., Poulain, L., Gherzi, V., Rodriguez, E.,

Beirle, S., Zotter, P., von der Weiden-Reinmuller, S. L., Bressi, M., Fountoukis, C., Petetin, H., Szidat, S. Schneider, J., Rosso, A., El Haddad, I., Megaritis, A., Zhang, Q. J., Michoud, V., Slowik, J. G., Moukhtar, S., Kolmonen, P., Stohl, A., Eckardt, S., Borbon, A., Gros, V., Marchand, N., Jaffrezo, J. L., Schwarzenboeck, A., Colomb, A., Wiedensohler, A., Borrmann, S., Lawrence, M., Baklanov, A., and Baltensperger, U. (2015). In-situ, satellite measurement and model evidence for a dominant regional contribution to fine particulate matter levels in the Paris Megacity, *Atmospheric Chemistry and Physics Discussions*, 15, 8647-8686.

Couvidat, F., Kim, Y., Sartelet, K., Seigneur, C., Marchand, N., and Sciare, J. : Modeling secondary organic aerosol in an urban area: Application to Paris, France, *Atmos. Chem. Phys.*, 13, 983-996, 2013.

Crippa, M., DeCarlo, P. F., Slowik, J. G., Mohr, C., Heringa, M. F., Chirico, R., Poulain, L., Freutel, F., Sciare, J., Cozic, J., Di Marco, C. F., Elsasser, M., Nicolas, J. B., Marchand, N., Abidi, E., Wiedensohler, A., Drewnick, F., Schneider, J., Borrmann, S., Nemitz, E., Zimmermann, R., Jaffrezo, J.-L., Prévôt, A. S. H., and Baltensperger, U.: Wintertime aerosol chemical composition and source apportionment of the organic fraction in the metropolitan area of Paris, *Atmos. Chem. Phys.*, 13, 961-981, doi:10.5194/acp-13-961-2013, 2013a.

Crippa, M., Canonaco, F., Slowik, J. G., El Haddad, I., DeCarlo, P. F., Mohr, C., Heringa, M. F., Chirico, R., Marchand, N., Temime-Roussel, B., Abidi, E., Poulain, L., Wiedensohler, A., Baltensperger, U., and Prévôt, A. S. H.: Primary and secondary organic aerosol origin by combined gas-particle phase source apportionment, *Atmos. Chem. Phys.*, 13, 8411-8426, doi:10.5194/acp-13-8411-2013, 2013b.

Crippa, M., Haddad, I., Slowik, J., DeCarlo, P., Mohr, C., Heringa, M., Chirico, R., Marchand, N., Sciare, J., Baltensperger, U. and Prévôt, A.: Identification of marine and continental aerosol sources in Paris using high resolution aerosol mass spectrometry, *J. Geophys. Res.*, 118, 1950–1963, doi:10.1002/jgrd.50151, 2013c.

Freutel, F., Schneider, J., Drewnick, F., von der Weiden-Reinmüller, S.-L., Crippa, M., Prévôt, A. S. H., Baltensperger, U., Poulain, L., Wiedensohler, A., Sciare, J., Sarda-Estève, R., Burkhardt, J. F., Eckhardt, S., Stohl, A., Gros, V., Colomb, A., Michoud, V., Doussin, J. F., Borbon, A., Haeffelin, M., Morille, Y., Beekmann, M., and Borrmann, S.: Aerosol particle measurements at three stationary sites in the megacity of Paris during summer 2009: meteorology and air mass origin dominate aerosol particle composition and size distribution, *Atmos. Chem. Phys.*, 13, 933-959, doi:10.5194/acp-13-933-2013, 2013.

Michoud, V., Kukui, A., M. Camredon, A. Colomb, A. Borbon, K. Miet, B. Aumont, M. Beekmann, R. Durand-Jolibois, S. Perrier, P. Zapf, G. Siour, W. Ait-Helal, N. Locoge, S. Sauvage, C. Afif, V. Gros, M. Furger, G. Ancellet, and J. F. Doussin: Radical budget analysis in a suburban European site during the MEGAPOLI summer field campaign, *Atmos. Chem. Phys.*, 12, 11951-11974, 2012.

Randerson, J., Chen, Y., Werf, G., Rogers, B. and Morton, D.: Global burned area and biomass burning emissions from small fires, *J. Geophys. Res.*, 117, doi:10.1029/2012JG002128, 2012.

Skyllakou, K., Murphy, B. N., Megaritis, A. G., Fountoukis, C., and Pandis, S. N.: Contributions of local and regional sources to fine PM in the megacity of Paris, *Atmos. Chem. Phys.*, 14, 2343-2352, doi:10.5194/acp-14-2343-2014, 2014.

Zhang, Q. J., Beekmann, M., Drewnick, F., Freutel, F., Schneider, J., Crippa, M., Prevot, A. S. H., Baltensperger, U., Poulain, L., Wiedensohler, A., Sciare, J., Gros, V., Borbon, A., Colomb, A., Michoud, V., Doussin, J.-F., Denier van der Gon, H. A. C., Haefelin, M., Dupont, J.-C., Siour, G., Petetin, H., Bessagnet, B., Pandis, S. N., Hodzic, A., Sanchez, O., Honoré, C., and Perrussel, O.: Formation of organic aerosol in the Paris region during the MEGAPOLI summer campaign: evaluation of the volatility-basis-set approach within the CHIMERE model, *Atmos. Chem. Phys.*, 13, 5767-5790, doi:10.5194/acp-13-5767-2013, 2013.

Responses to the Comments of Referee #3

(1) The scope of the paper appears to be a little narrower than promised by the title. We do agree with the point of the reviewer. The title of the paper has been changed to “In situ formation and spatial variability of particle number concentration in a European Megacity”, which better describes the final scope of this paper.

(2) The ambiguity in definition of ultrafine particles (with the air pollution community, policymakers and regulators referring to traffic-dominated Aitken mode particles finer than about 100 nm as ultrafine) could be addressed with modest modification to the title and short clear description of the scope of the current study. Such a definition section within the introduction would definitely benefit the special issue. Between the first and second paragraphs of the introduction (i.e. between the PM_{2.5} and NPF related sections) or between the third and fourth paragraphs (linking and contextualizing in situ emission and in situ formation contributions) might be appropriate places.

The title has been changed and it does not include anymore a reference to ultrafine particles. We do agree with the reviewer that it can be confusing. The paragraph describing the scope of this study has been slightly modified stressing that the periods under investigation correspond to the two extreme conditions (frequent new particle formation-clean conditions and infrequent new particle formation-polluted conditions) encountered in the Paris region.

(3) The companion paper in the special issue from the same group (Skylakou et al., 2014) addressing the sources of "fine" particles, defined therein as PM_{2.5}, carries out a more conventionally defined (though quite novel) source attribution study. Challenges to performing such a comparable source attribution for the ultrafines should be discussed

This is a good point. Source attribution of particle number concentrations is challenging because particle number is not conserved due to coagulation and the particle size distribution is modified due to condensation/evaporation, nucleation, and removal. There are a few efforts in the literature trying to estimate the sources of the particle number (Wählén et al., 2001; Houssein et al., 2004; Zhou et al., 2005; Chan and Mozurkewich, 2007). One method that has been applied is Positive Matrix Factorization which unfortunately cannot account for new particle formation. In order to apply such methods periods of new particle formation should be omitted (Zhou et al., 2005). This corresponds to half of the Paris summer campaign dataset. There has been an effort by our team recently (Posner and Pandis, 2015) to perform such particle number source attribution based on the results of a Chemical Transport Model. This produced encouraging results for particles smaller than 100 nm, but had weaknesses for larger particles. We have added a paragraph in the revised manuscript discussing these issues.

(4) It is difficult to consider attribution of NPF by source if there is no simultaneous source attribution of condensation sink. The authors might like to expand on the outlook for resolving NPF mechanisms and sources in complex environments, with significant mixing of air masses from different sources at a range of scales.

Our hypothesis was that we would be able to explore the spatial variability of new particle formation in the complex environment in and around a Megacity to learn more about the corresponding mechanisms. While we did observe variability in space

(please Section 7 and Figure 2), we could not relate it to any of the measured species. This does show that there are opportunities in these complex environments, but additional measurements of candidate nucleating vapors are required. The condensational sink can be viewed as an obstacle to nucleation. For these urban environments the condensational sink correlates reasonable well with PM1 or PM2.5 and the source attribution of the corresponding mass concentrations can be used as a reasonable proxy. The source contributions to fine PM for the MEGAPOLI campaigns have been discussed in detail by Beekmann et al. (2015). A brief discussion of these points has been added to the revised manuscript.

(5) I am in some agreement that broader consideration of material other than number and size measurements would provide more insight. This may be possible by reference to other papers in the special issue

Additional references to the related source apportionment work during the same field studies have been added.

References

Beekmann, M., Prévôt, A. S. H., Drewnick, F., Sciare, J., Pandis, S. N., Denier van der Gon, H. A. C., Crippa, M., Freutel, F., Poulain, L., Gherzi, V., Rodriguez, E., Beirle, S., Zotter, P., von der Weiden-Reinmuller, S. L., Bressi, M., Fountoukis, C., Petetin, H., Szidat, S. Schneider, J., Rosso, A., El Haddad, I., Megaritis, A., Zhang, Q. J., Michoud, V., Slowik, J. G., Moukhtar, S., Kolmonen, P., Stohl, A., Eckardt, S., Borbon, A., Gros, V., Marchand, N., Jaffrezo, J. L., Schwarzenboeck, A., Colomb, A., Wiedensohler, A., Borrmann, S., Lawrence, M., Baklanov, A., and Baltensperger, U. (2015). In-situ, satellite measurement and model evidence for a dominant regional contribution to fine particulate matter levels in the Paris Megacity, *Atmospheric Chemistry and Physics Discussions*, 15, 8647-8686.

Chan, T. and Mozurkewich, M.: Application of absolute principal component analysis to size distribution data: identification of particle origins, *Atmos. Chem. Phys.*, 7, 887–897, doi:10.5194/acp-7-887-2007, 2007.

Hussein, T., Puustinen, A., Aalto, P., Mäkelä, J., Hämeri, K. and Kulmala, M.: Urban aerosol number size distributions, *Atmos. Chem. Phys.*, 4, 391–411, doi:10.5194/acp-4-391-2004, 2004.

Posner, L. N. and Pandis S. N.: Sources of ultrafine particles in the Eastern United States, *Atmos. Environ.*, 111, 103-112, 2015.

Wählin, P.: Measured reduction of kerbside ultrafine particle number concentrations in Copenhagen, *Atmos. Environ.*, 43, 3645–3647, 2009.

Zhou, L., Kim, E., Hopke, P., Stanier, C. and Pandis, S. N. : Advanced factor analysis on Pittsburgh particle size-distribution data, *Aerosol Sci. and Technol.*, 38 (Suppl. 1), 118-132, doi:10.1080/02786820390229589, 2004.

Ultrafine particle sources and in-situ formation and spatial variability of particle number concentration in a European Megacity

Michael Pikridas^{1,2,3}, Jean [Sciare^{3,4}Sciare^{4,3}](#), [Friederike Freutel⁵](#), [Suzanne Crumeyrolle^{6*}](#),
Sarah-Lena von der Weiden-Reinmüller⁵, [Suzanne Crumeyrolle⁴](#), [Friederike Freutel⁵](#),
Agnes [Borbon⁶Borbon⁷](#), Alfons [Schwarzenboeck⁴Schwarzenboeck⁶](#), Maik
[Merkel⁷Merkel⁸](#), Monica [Crippa⁸Crippa⁹](#), Evangelia Kostenidou^{1,2}, Magda Psychoudaki^{1,2},
Lea [Hildebrandt⁹Hildebrandt¹⁰](#), Gabriella J. [Engelhart⁹Engelhart¹⁰](#), Tuukka
[Petäjä¹⁰Petäjä¹¹](#), Andre S. H. [Prevot⁸Prévôt⁹](#), Frank Drewnick⁵, Urs
[Baltensperger⁸Baltensperger⁹](#), Alfred [TWiedensohler⁷Wiedensohler⁸](#), Markku
[Kulmala¹⁰Kulmala¹¹](#), Matthias [Beekmann⁶Beekmann⁷](#), and Spyros N. Pandis^{1,2,9,10}

¹Department of Chemical Engineering, University of Patras, Greece

²Institute of Chemical Engineering Sciences (ICEHT), FORTH, Patras, Greece

³The Cyprus Institute, Environment Energy and Water Resources Center, Nicosia, Cyprus

⁴[Laboratoire Meteorologie Physique \(LaMP\), 24 avenue des Landais, 63177, Aubiere, France](#)

⁴[Laboratoire des Sciences du Climat et de l'Environnement \(LSCE\), Gif/Yvette, France](#)

⁵Max Planck Institute for Chemistry, Particle Chemistry Department, Mainz, Germany

⁶[Laboratoire Meteorologie Physique \(LaMP\), 24 avenue des Landais, 63177, Aubiere, France](#)

⁷[Laboratoire Interuniversitaire des Systemes Atmospheriques, CNRS, Universites Paris-Est & Paris Diderot, 61 av. Du Gal de Gaulle, 94010 Creteil, France](#)

⁷[Leibniz⁸Leibniz](#) Institute for Tropospheric Research, Leipzig, Germany

⁸[Paul⁹Paul](#) Scherrer Institute, Laboratory of Atmospheric Chemistry, Villigen, Switzerland

⁹[Department of](#) ¹⁰[Department of](#) Chemical Engineering, Carnegie Mellon University, Pittsburgh, USA

¹⁰[Department of](#) ¹¹[Department of](#) Physics, University of Helsinki, Helsinki, Finland

^{*} [now at LOA, UMR8518, CNRS – Université Lille1, Villeneuve d'Ascq, France](#)

Abstract

Ambient particle number size distributions were measured in Paris, France during summer (1 - 31 July 2009) and winter (15 January – 15 February 2010) at three fixed ground sites and using two mobile laboratories and one airplane. The campaigns were part of the MEGAPOLI project. New particle formation (NPF) was observed only during summer at approximately 50% of the campaign days, assisted by the low condensation sink (about $10.7 \pm 5.9 \times 10^{-3} \text{ s}^{-1}$). NPF events inside the Paris plume were also observed at 600 m altitude onboard an aircraft simultaneously with regional events identified on the ground.

39 Increased particle number concentrations were measured aloft also outside of the Paris
40 plume at the same altitude, and were attributed to NPF. The Paris plume was identified,
41 based on increased particle number and black carbon concentration, up to 200 km away
42 from Paris center during summer. The number concentration of particles with diameter
43 exceeding 2.5 nm measured on the surface at Paris center was on average $6.9 \pm 8.7 \times 10^4 \text{ cm}^{-3}$
44 and $12.1 \pm 8.6 \times 10^4 \text{ cm}^{-3}$ during summer and winter, respectively, and was found to decrease
45 exponentially with distance from Paris. However, further than 30 km from the city center,
46 the particle number concentration at the surface was similar during both campaigns.
47 During summer one suburban site in the NE was not significantly affected by Paris
48 emissions due to higher background number concentrations, while the particle number
49 concentration at the second suburban site in the SW increased by a factor of three when it
50 was downwind of Paris.

51

52 **1. Introduction**

53 Urban areas in the developed and developing world have been growing annually by
54 0.7% in population since 2005 and comprised approximately 54% of the total population of
55 the planet in 2014 (United Nations, 2014). In this work, following the definition of the
56 Organization for Economic Co-operation and Development (OECD), urban areas are
57 defined as corresponding to a population density greater than 1500 inhabitants per km^2
58 (OECD, 2013). Several of these urban areas have increased in size to mega-centers,
59 attracting more than 10 million inhabitants. This has led to an increasing demand for
60 transportation, energy and industrial activity, which resulted in concentrated emission of
61 gases and particulate matter (PM) impacting local air quality (Molina and Molina, 2004;
62 Molina et al., 2004; Lawrence et al., 2007; Gurjar et al., 2008). Several epidemiological
63 studies suggest that the risk of cancer, particularly lung cancer, is increased for people
64 residing in areas affected by urban air pollution (Barbone et al., 1995; Beeson et al., 1998;
65 Laden et al., [20012006](#); Nyberg et al., 2000; Pope et al., 2002; Nafstad et al., 2003). Pope
66 et al. (2009) and Wang et al. (2008) showed that fine particles with diameter smaller than
67 $2.5 \mu\text{m}$ ($\text{PM}_{2.5}$) are related to increased mortality.

68 Aerosol particles can change climate patterns and the hydrological cycle on regional
69 and global scales (Chung et al., 2005; Lohmann and Feichter, 2005; IPCC, 2007).
70 Submicrometer particles, down to 100 nm, are the most effective ones in scattering solar
71 radiation. The uncertainties in the primary emission rates of these pollutants and in their

72 formation from gaseous precursors are still large. On a global scale new particle formation
73 (NPF), that is nucleation of low volatility vapors and subsequent condensational growth to
74 larger sizes, is the major reason for high particle number concentrations_ (Kulmala et al.,
75 2004). The mechanism behind this major particle formation process is still not completely
76 understood (Riccobono et al., 2014). This uncertainty has a direct impact on our
77 understanding of the role of nucleated particles in climate change (Pierce and Adams,
78 2009). NPF is often a regional phenomenon covering areas of several hundred square
79 kilometers (Vana et al., 2004; Stanier et al., 2004a; Komppula et al., 2006; Crumeyrolle et
80 al., 2010) but it can be space-restricted when the source of one of the nucleating vapors is
81 space limited, as it has been observed in coastal sites (Wen et al., 2006).

82 During the past decade a number of studies reported ambient particle number
83 concentrations in urban areas. The measurement period spanned from a few months
84 (Hering et al., 2007; Wang et al., 2010; Dunn et al., 2004; Baltensperger et al., 2002;
85 McMurry et al., 2005), to one or more years (Woo et al., 2001; Alam et al., 2003; Shi,
86 2003; Wehner and Wiedensohler, 2003; Stanier et al., 2004b; Wehner et al., 2004; Wu et
87 al., 2007; Rodriguez et al., 2005; Watson et al., 2006; Wählín, 2009). The majority of
88 studies are based on observations from one or at most two stationary sites, assuming that
89 these stations are representative of the area under investigation. Most of these studies have
90 found higher concentrations during winter due to both increased emissions caused by
91 higher energy demand, and lower boundary layer height. Also, typically a diurnal pattern
92 has been found that shows peaks due to morning rush hour traffic during weekdays but not
93 on weekends.

94 NPF has often been observed in urban areas (Woo et al., 2001; Baltensperger et al.,
95 2002; Laakso et al., 2003; Tuch et al., 2003; Stanier et al., 2004a; Watson et al., 2006; Wu
96 et al., 2007), but growth and nucleation rates are rarely reported in these studies (Birmili
97 and Wiedensohler, 2000; McMurry, 2000; Shi et al., 2007; Wehner et al., 2007; Manninen
98 et al., 2010).

99 During the “Megacities: Emissions, urban, regional and Global Atmospheric
100 POLLution and climate effects, and Integrated tools for assessment and mitigation”
101 (MEGAPOLI) project (Baklanov et al., 2010), measurements were conducted in and
102 around the megacity of Paris. Gas and particulate phase measurements from three fixed
103 ground sites, two mobile laboratories, and one airplane were collected for both summer
104 2009 and winter 2010. The residence time of the air mass over land was found to influence
105 PM mass levels, with longer residence times leading to higher PM levels mass

106 | [concentrations](#) (Freutel et al., 2013). [As a result air](#) Air masses from the Atlantic, which
107 | were dominating during the summer campaign, led to relatively clean conditions (Freutel
108 | et al., 2013; Freney et al., 2014). Cooking was identified as a significant local [organic](#)
109 | [aerosol](#) source within Paris during summer with vehicular traffic being second (Crippa et
110 | al., 2013b). During winter [residential](#) wood burning [for residential purposes](#) was found to
111 | be a major source of [primary particulate matter](#) organic aerosol (Crippa et al., 2013a).
112 | [During both MEGAPOLI campaigns, the contribution of primary transportation emissions](#)
113 | [to submicrometer organic aerosol \(OA\) was around 6% \(Crippa et al., 2013b\). In the year](#)
114 | [of the MEGAPOLI campaigns, 61% of the light duty vehicles in France were powered by](#)
115 | [diesel engines and 72% of the consumed fuel was diesel \(World Bank, 2012\). The sulfur](#)
116 | [content of diesel in France at that time was 10 ppm compared for example to 500 ppm in](#)
117 | [1998. The sulfur content of fuel affects both the total particle emissions but also the shape](#)
118 | [of the corresponding aerosol distribution \(Platt et al., 2013; Bermúdez et al., 2015\).](#)

119 | [Beekmann et al. \(2015\) have presented a synthesis of the MEGAPOLI PM mass](#)
120 | [source attribution efforts based on the corresponding field measurements. In parallel,](#)
121 | [several modeling efforts have been also conducted examining the contribution of regional](#)
122 | [sources to fine PM \(Skylakou et al., 2014\) and investigating the organic aerosol sources in](#)
123 | [Paris \(Couvidat et al., 2013; Zhang et al., 2013\). All of these studies focused on PM mass](#)
124 | [concentration and not on particle number. The different size distributions of the aerosol](#)
125 | [emitted by different sources usually result in very different source contributions to particle](#)
126 | [number and mass \(Zhou et al., 2004\). There have been a number of studies that tried to](#)
127 | [quantify the particle number sources using available size distribution measurements](#)
128 | [\(Wählín et al., 2001; Hussein et al., 2004; Zhou et al., 2004; Chan and Mozurkewich,](#)
129 | [2007\). However, the changes of these distributions due to new particle formation and](#)
130 | [growth or other dynamic changes seriously limit the applicability of techniques like](#)
131 | [Positive Matrix Factorization \(PMF\). Zhou et al. \(2004\) excluded the corresponding new](#)
132 | [particle formation periods from their dataset to overcome this problem.](#)

133 | In this work we focus on the particle number concentrations in Paris and its
134 | surroundings during both (summer and winter) campaigns. The effect of the Paris megacity
135 | on the downwind areas [will be](#) assessed together with the spatial extent of its influence.
136 | The frequency and spatial characteristics of new particle formation events are [also](#)
137 | investigated.

138 | 2. Sampling sites

139 |

140 Month long campaigns were conducted in the Parisian region during summer (1 July
141 to 31 July 2009) and winter (15 January to 15 February 2010). They included monitoring
142 of the aerosol size distribution along with composition, coupled with gas phase and
143 meteorological monitoring.

144 The city of Paris is an urbanized area covering about 3000 km² with 2.2 million
145 inhabitants. The greater Paris area, called Île de France (IDF), is one of the largest
146 metropolitan areas in Europe including more than 12 million inhabitants. The
147 administrative boundaries of Paris and IDF are shown in Fig. 1 along with the population
148 density map of the area.

149 Detailed aerosol particle measurements were conducted at an urban and two sub-
150 urban sites (Fig. 1). The Site Instrumental de Recherche par Télédétection Atmosphérique
151 (SIRTA, 48° 43' 5" N and 2° 12' 26" E) is located on the campus of Ecole Polytechnique
152 (Palaiseau), 20 km southwest of Paris center in a semi-urban environment inside the
153 campus of Ecole Polytechnique. This site is surrounded by highways at 3-6 km distance in
154 all wind directions. Measurements in the Laboratoire d'Hygiène de la Ville de Paris
155 (LHVP, 48° 49' 11" N and 2° 21' 35" E), inside of Paris, were performed on a terraced
156 roof 14 m above ground level and on the ground inside a research container. This site
157 includes a station of the AIRPARIF air quality monitoring network and is representative of
158 the Paris urban background air pollution (Sciare et al., 2010; Favez et al., 2007). Finally
159 the sub-urban station at Golf de la Poudrerie (GOLF, 48° 56' 2" N and 2° 32' 49" E) was
160 located 20 km northeast of Paris center near a golf course and a forested park.

161 Two mobile platforms, named "MoLa" (Mobile Laboratory) and "MOSQUITA"
162 (Measurements Of Spatial QUantitative Immissions of Trace gases and Aerosols), were
163 operated by the Max Planck Institute for Chemistry (Drewnick et al., 2012; von der
164 Weiden-Reinmüller et al., 2014a) and the Paul Scherrer Institute (Bukowiecki et al., 2002;
165 Weimer et al., 2009), respectively. The measurement path of both mobile platforms was
166 decided based on forecasts of the chemical transport model CHIMERE (Rouil et al., 2009;
167 Menut and Bessagnet, 2010; Menut et al., 2013). Three measurement strategies were
168 employed during both campaigns: stationary, axial and cross sectional measurements (von
169 der Weiden-Reinmüller et al., 2014a; 2014b). Cross sectional (mobile) measurements were
170 carried out by maintaining approximately constant distance from Paris center while
171 varying the cardinal directions, allowing distinction between background concentrations
172 and Paris emissions. Axial (mobile) measurements were conducted by maintaining
173 approximately the same cardinal direction while varying the distance with respect to Paris

174 center, thus monitoring the evolution of the plume. Stationary measurements were
175 conducted when the direction of the Paris emissions, based on the CHIMERE model, were
176 not stable enough to allow cross sectional or axial measurements. Stationary measurements
177 were conducted only by MoLa either downwind of Paris, or upwind to assess background
178 aerosol loadings.

179 The airborne measurements were performed by an ATR-42 and a Piper Aztec aircraft
180 during summer and winter, respectively, operated by the French Service des Avions
181 Français Instrumentés pour la Recherche en Environnement (SAFIRE). Each flight
182 included a circle around IDF followed by crossing the expected Paris plume multiple
183 times, at a constant altitude of 600 and 500 m above sea level for the summer and winter
184 campaigns, respectively. During July 1 the flight path was kept at a constant altitude of
185 approximately 800 m. Flights were performed on 11 out of the 31 days of the summer
186 campaign. Fig. 2 shows the flight patterns and sampling days of the ATR-42 during
187 summer. Flight days were selected based on CHIMERE predictions. Higher PM
188 concentration days were favored, thus the observed aerosol properties are expected to be
189 biased toward more polluted conditions. During winter two flights per sampling day were
190 conducted for four days (January 27 and 31, February 14 and 15). The first flight included
191 a survey of the aerosol properties around IDF and the second monitored the Paris plume,
192 following a flight path similar to the summer one.

193

194

195 **2.1 Instrumentation**

196 The MEGAPOLI project focused on the properties of ambient aerosol, including
197 both mass and number concentration measurements. This work examines the particle
198 number concentration N during both MEGAPOLI campaigns; the instruments and
199 measurements relevant for this purpose are summarized in Table 1. [A number of additional
200 measurements of concentrations of gas-phase pollutants, radicals, etc., were conducted
201 during the campaigns \(Michoud et al., 2012\), but are not used in the present work because
202 they did not provide any additional insights.](#)

203 At SIRTA, [threetwo](#) instruments were used to monitor the ambient particle number
204 distribution. A Scanning Mobility Particle Sizer (SMPS; TSI Model 3936) sampled aerosol
205 particles from 10 to 500 nm in diameter through an inlet located approximately at 4 m
206 above ground. The particles were actively dried using a Nafion dryer. [An Air Ion](#)

207 [Spectrometer \(AIS; Mirme et al., 2007\) monitored the size distribution of ambient \(not](#)
208 [dried\) positive and negative air ions of mobility diameters ranging from 0.8 to 40 nm. To](#)
209 [minimize particle losses the sampling line length of the AIS was 30 cm.](#) A Differential
210 Mobility Particle Sizer (DMPS, Aalto et al., 2001) [also](#) monitored, [close to the AIS,](#)
211 ambient number size distributions ranging from 6 to 800 nm [during summer](#). At LHVP, the
212 sampling inlet was located 6 m above ground and the aerosol sample was dried using a
213 diffusion dryer as described in Tuch et al. (2009) before entering a mobility particle size
214 spectrometer TROPOS-type TDMPS (Twin Differential Mobility Particle Sizer; Birmili et
215 al., 1999), which monitored the aerosol size distribution from 3 to 630 nm. [At the same](#)
216 [site, an Air Ion Spectrometer \(AIS; Mirme et al., 2007\) monitored the size distribution of](#)
217 [ambient \(not dried\) positive and negative air ions of mobility diameters ranging from 0.8 to](#)
218 [40 nm. To minimize particle losses the sampling line length of the AIS was 30 cm.](#) At
219 GOLF, the particle size distribution between 5 nm and 1 μm was monitored with an
220 Electrical Aerosol Spectrometer (EAS, Airel Ltd.) and sampling was conducted 8 m above
221 ground. Because the three aerosol size distribution instruments (SMPS, TDMPS, EAS)
222 used for the stationary ground measurements during both campaigns overlaps between 10
223 nm and 500 nm (mobility diameter), our analysis will focus on this size range, denoted as
224 N_{10-500} .

225 MoLa, which was based at GOLF, monitored the total particle number concentration
226 via an Ultrafine Water Condensation Particle Counter (UWCPC, TSI Model 3786) with
227 50% detection efficiency at 2.5 nm, which will be denoted as $N_{2.5}$. The aerosol inlet during
228 stationary measurements was located at approximately the same height as the stationary
229 measurements at GOLF (8 m above ground). During mobile measurements, sampling
230 occurred at about 2.4 m above ground level. MOSQUITA monitored the total particle
231 number concentration via a butanol-based Condensation Particle Counter (CPC; TSI
232 Model 3010, 50% detection efficiency at 10 nm) during summer, further denoted as N_{10} ,
233 and via an Ultra High Sensitivity Aerosol Spectrometer (UHSAS; DMT Model A) during
234 winter. The UHSAS monitored the size distribution, with respect to the optical diameter,
235 ranging from 60 nm to 1 μm .

236 On-board the METEO-FRANCE aircraft (ATR-42), aerosols were sampled, under
237 dry conditions, through the community aerosol inlet ([Gomes et al., 2014](#)) and delivered to
238 a comprehensive suite of aerosol instruments. This isokinetic and isoaxial inlet is based on
239 the University of Hawaii shrouded solid diffuser designed by A. Clarke and had been
240 modified by Meteo France (McNaughton et al., 2007). Particle number concentration was

241 monitored directly during summer and winter flights using a CPC with 10 nm (TSI Model
242 3010) and 2.5 nm (TSI Model 3025) lower cutoff, respectively. Because the CPCs used
243 during the summer and winter campaigns had different lower detection limits, the
244 corresponding number concentrations will be denoted as N_{10} and $N_{2.5}$, respectively.

245 In order to quantify potential differences between instruments, at least one of the
246 mobile laboratories visited each site for 5-15 hours during each campaign. During summer,
247 the differences in number concentration between the CPC on board the visiting mobile
248 laboratory (MOSQUITA) and the aerosol sizing instrument at each of the stationary sites
249 did not exceed 10% (Figure S1 in the Supplementary Information). The CPC on board
250 MOSQUITA had a detection size limit equal to approximately 10 nm. During winter the
251 MoLa CPC, with a lower detection size limit of 2.5 nm, was employed for the
252 intercomparisons. In this case, the differences were higher and equal to 30%, 18%, and
253 19% at SIRTA, LHVP, and GOLF, respectively. Taking into account that particles below
254 10 nm were typically present at SIRTA during winter the corresponding discrepancy can
255 be partially explained by the different detection limits of the two instruments (10 nm for
256 the SMPS at SIRTA and 2.5 nm for the MoLa CPC). During both campaigns the number
257 concentrations monitored onboard MoLa and MOSQUITA were also compared for
258 approximately 8 hours. The two instruments were found to agree when the concentrations
259 of the nucleation mode particles were moderate or low. This is expected due to their
260 different size detection limits. The results of this intercomparison have been presented by
261 von der Weiden-Reinmüller et al. (2014a).

263 3. Methods

264 3.1 Particle formation event categorization

265 Particle formation events have been categorized in the past based on the
266 concentration of 1.6 – 7.5 nm air ions (Hiirsiko et al., 2007; Vana et al., 2008) and on the
267 concentration of total ambient particles below 25 nm (Stanier et al., 2004a; Dal Maso et al.,
268 2005). At [SIRTA LHVP](#) both air ions and ambient particles were measured and therefore
269 we used two classification schemes, one based solely on ambient particles following Dal
270 Maso et al. (2005) and one that includes air ions, following Hirsikko et al. (2007). In both
271 cases, the observation period was divided into particle formation event days, non-event
272 days and undefined days. In general, a day is classified as event day if a nucleation mode
273 (particles with sizes smaller than 10 nm) is present for several hours and grows

274 continuously during the course of the day. If no traces of a nucleation mode are seen, a day
275 is classified as a non-event day. Days that did not clearly belong to either of the
276 aforementioned categories were classified as undefined. Examples of event, undefined and
277 non-event days are shown in Figs. 3, 4 and 5, respectively.

278 During July 12, a nucleation mode appeared at 14:00 LST (local standard time)
279 simultaneously at all ground sites (Fig. 3). During this cloudy day, nucleation was
280 observed approximately one hour after the solar intensity increased by a factor of three
281 (from 300 to 1070 W m⁻²). This day was consequently classified as event day. During July
282 10, an increase in the number concentration of particles above 10 nm in diameter was
283 measured simultaneously at LHVP and SIRTA at 14:00 LST (Fig. 4). It was unclear
284 whether the mode also appeared at GOLF due to interferences by local sources. Particle
285 growth was not continuous and the mode disappeared abruptly after approximately three
286 hours, even though the direction of the wind did not change at this time. At [SIRTA](#)[LHVP](#)
287 air ion bursts in the size range between 1.6 – 7.5 nm did not follow a distinct pattern but
288 were random. As a result it was unclear whether NPF occurred and the day was classified
289 as undefined for all sites. During July 29, no nucleation event was observed, and the day
290 [was](#) consequently classified as non-event day. During this day, the condensation sink (CS)
291 was rather high ($9.0 \pm 1.7 \times 10^{-3} \text{ s}^{-1}$, $20.3 \pm 9.7 \times 10^{-3} \text{ s}^{-1}$ and $14.4 \pm 4.1 \times 10^{-3} \text{ s}^{-1}$ at SIRTA, LHVP
292 and GOLF respectively) from 08:00 to 16:00 LST, when NPF was expected to occur.
293 These sink values were above the summer average for all sites (see Section 3.3) and
294 contributed to the lack of a nucleation mode at all sites (Fig. 5).

295

296 **3.2 Duration of nucleation events**

297 The duration of nucleation events at [SIRTA](#)[LHVP](#) was calculated based on AIS
298 measurements following the procedure described by Hirsikko et al. (2005) and Pikridas et
299 al. (2012). In brief, a normal distribution was fitted to the time series of concentration of
300 air ions with diameters between 2 and 5 nm. The beginning of the event was determined by
301 the initial increase of the air ion concentration (assuming a stable air ion concentration
302 before the event) and the end by the peak of the normal distribution. A decrease of the
303 number concentration implies that the rate of particle production is lower than the
304 combined rates of coagulation and particle growth to diameters greater than 5 nm, or that
305 the air mass is getting diluted; it does not necessarily imply that the rate of production is
306 zero. Our calculated event-end is thus a lower bound estimate.

307

3.3 Condensation sink

The condensation sink (CS) is defined as the condensational loss rate constant of vapors (Kulmala et al., 2001; Dal Maso et al., 2002). The CS values were calculated based on the aerosol number size distribution using:

$$CS = 2\pi D \int_0^{\infty} D_p \beta_m(D_p) n(D_p) dD_p = 2\pi D \sum_i D_{pi} \beta_{mi} N_i \quad (1)$$

where D is the diffusion coefficient of the condensing vapor, D_{pi} is the diameter and N_i the particle number concentration in size class. The term β_{mi} corresponds to the transition regime correction factor for the size class i , which was calculated based on Fuchs and Sutugin (1971). The properties of the condensable vapors are assumed to be similar to those of sulfuric acid, without accounting for hydration, leading to an upper limit estimate. If the aerosol sample was dried prior to the measurement, the diameter reduction due to water loss was estimated using the Extended Aerosol Inorganic Model II (E-AIM, http://www.aim.env.uea.ac.uk/_aim/aim.php; Carslaw et al., 1995; Clegg et al., 1998; Massucci et al., 1999). The hourly averaged inorganic concentrations for sulfate, ammonium and nitrate measured by the aerosol mass spectrometer (AMS; Jayne et al., 2000; Jimenez et al., 2003) and ambient RH measured at each site, were used as inputs to the model, neglecting any contribution of organics to the aerosol water content. The volume growth factor was determined following the method of Engelhart et al. (2011) which assumes that all submicrometer particles grow similarly by neglecting the Kelvin effects. The diameter growth factor was calculated as the cubic root of the volume growth factor and was applied to the whole particle distribution.

3.4 Mobile measurements

Due to the high frequency of local contamination events, mobile data was post-processed by examining video footage recorded at the driver's cabin of the mobile laboratory, based on Drewnick et al. (2012). Measurement periods were omitted from analysis if traffic was identified less than 150 m from the platform; if human activities (e.g. cooking, heating) were spotted; when driving at low speed caused a possible contamination by the vehicle's own exhaust; and when travelling inside tunnels. In order to reduce the amount of contaminated data major roads were avoided. More details concerning the conditioning of mobile measurements presented in this study can be found in von der Weiden-Reinmüller et al. (2014a). Further analysis of the mobile dataset was conducted based on results from

340 the particle dispersion model FLEXPART performed in forward mode (Stohl et al., 2005).
341 Particles were released from an area whose borders were determined by the population
342 density map presented on Fig. 1 and included Paris. Based on these modeling results and
343 the respective measurement tracks, mobile measurements were attributed as influenced or
344 not by Paris emissions.

345

346 **4. Meteorology**

347 During summer, the lowest ambient temperature was 12°C, observed at SIRTA and
348 GOLF, and the highest of 33°C was measured at LHVP. Campaign average temperatures
349 during summer were 19.7, 21.1 and 18.7 °C at GOLF, LHVP and SIRTA, respectively. In
350 general, the temperature was higher inside the city center by 1°C at least, compared to the
351 suburban sites. Diurnal variations of RH (ranging from 35% to 90%) and temperature were
352 similar at all sites during summer. There were several cloudy periods and cloud coverage
353 was geographically dependent. During summer at all ground sites, solar radiation reached a
354 maximum of 900 W m⁻² while the presence of clouds could reduce it by a factor of three.
355 Precipitation as monitored at SIRTA occurred on 8 of the 31 days of the campaign (July 8,
356 16-18, 22, 23, 27 and 30). Maximum observed precipitation rate during the summer
357 campaign was 0.5 mm min⁻¹; however it rarely exceeded 0.1 mm min⁻¹.

358 During winter the campaign average ambient temperatures were 2.6, 3.3 and 1.2 °C
359 at GOLF, LHVP, and SIRTA, respectively. RH varied from 40% to 90% and exceeded
360 95% on several occasions at all sites. Hourly average global solar irradiance did not exceed
361 400 W m⁻² during the winter campaign and did not exceed 100 W m⁻² on 14 of the 32 days
362 of observations. Precipitation occurred during winter on two [thirdthirds](#) (21 of 32 days) of
363 the campaign days and the average precipitation rate was approximately 0.15 mm min⁻¹.

364 Figure 6 shows the wind direction distribution at all sites, for each campaign. Wind
365 direction, measured at 10 m above ground, during summer was predominantly SW at
366 LHVP and GOLF and W at SIRTA (Fig. 6) indicating that air masses often crossed the city
367 center before reaching GOLF and that SIRTA was mostly upwind of the city. During
368 winter wind directions were more variable with the wind equally coming from both NE
369 and W (Fig 6). During the winter campaign SIRTA was more often than GOLF influenced
370 by air masses that crossed the urban area before reaching the site.

371

372

373 **5 Particle number concentrations and size distributions**

374 **5.1 Stationary measurements**

375 Average number concentrations of particles with diameters between 10 and 500 nm
376 (N_{10-500}), for all ground sites during both campaigns, are summarized in Table 2. On
377 average, the N_{10-500} concentrations during winter were higher than during summer by a
378 factor of two at SIRTA and GOLF, and by 35% at LHVP. The highest hourly averaged
379 concentrations were observed at GOLF ($54.1 \times 10^3 \text{ cm}^{-3}$ and $72.2 \times 10^3 \text{ cm}^{-3}$ during summer
380 and winter, respectively) followed by the urban center station LHVP ($34.4 \times 10^3 \text{ cm}^{-3}$ and
381 $45.5 \times 10^3 \text{ cm}^{-3}$ during summer and winter, respectively). The average ratio of the aerosol
382 number concentration observed at LHVP to the one observed at GOLF was 0.86 and 0.62
383 during summer and winter, respectively. The average ratio of the aerosol number
384 concentration observed at LHVP to the one observed at SIRTA was 2.1 and 1.5 during
385 summer and winter, respectively.

386 The particle number concentration at all sites followed the same diurnal pattern
387 during both seasons (Fig. 7). Regardless of site and season, minimum concentrations were
388 observed between 3:00 and 4:00 LST, when anthropogenic activities are expected to be
389 minimal. The concentration exhibited two maxima: during morning traffic hours, peaking
390 between 7:00 and 10:00 LST, and during nighttime, between 8:00 and 9:00 LST. These
391 diurnal profiles are typical of urban areas (Ruuskanen et al., 2001; Woo et al., 2001;
392 Watson et al., 2006).) and can be explained based on the evolution of the mixing layer
393 (Bukowiecki et al., 2005). In the afternoon atmospheric mixing reaches its maximum and
394 primary pollutant concentrations decrease due to dilution. The mixing height remains fairly
395 constant till nighttime when it decreases resulting in increasing primary pollutant levels.
396 Boundary layer measurements using a Cloud and Aerosol Micro Lidar (Cimel model CE-
397 370) at 355 nm that were performed at SIRTA support this explanation. The magnitude
398 and time of the peaks varied depending on site and season. By comparing these maxima,
399 which correspond to the peak of anthropogenic activity, against the minimum of the
400 diurnal cycle, a rough estimate of the N_{10-500} anthropogenic contribution can be made for
401 each site. During summer the increase was 84%, 79%, and 21% at GOLF, LHVP, and
402 SIRTA respectively, and during winter and 153%, 133% and 141%.

403 Average distributions for each season and site are shown in Fig. 8. During summer,
404 particles with diameter ranging from 30 to 100 nm dominated the N_{10-500} at SIRTA,
405 accounting on average for 53%, followed by particles with diameters ranging from 10 to
406 30 nm which accounted for 30% (Fig. 8). Similar behavior was observed at LHVP during
407 summer, where particles with diameter ranging from 30 to 100 nm accounted for 47% and
408 particles with diameters ranging from 10 to 30 nm for 40% of the N_{10-500} . However, N_{10-500}

409 measured at GOLF was dominated by particles with diameter ranging from 10 to 30 nm,
410 which accounted for 50% of the N_{10-500} , followed by particles with diameter ranging from
411 30 to 100 nm that accounted for 42%.

412 During winter the contribution of particles with diameter from 10 to 30 nm to N_{10-500}
413 was almost equal to that from particles with diameters 30 to 100 nm at SIRTA (42% and
414 39%, respectively) and LHVP (44% and 40%, respectively). At GOLF the contribution of
415 particles with diameters between 10 to 30 nm increased even further (compared to
416 summer) reaching 56%, and the contribution of particles with diameters between 30 to 100
417 nm decreased to 34%. These differences are due to the shift of the Aitken mode of the
418 distributions to lower sizes during the winter. Average size distributions for each site are
419 shown in Fig. 8, along with the corresponding lognormal modes. During summer, an
420 Aitken mode centered approximately at 35 nm was dominating the number distributions at
421 LHVP and SIRTA. Nucleated particles grew to approximately this size during summer
422 (see Fig. 3 and 4) and could be identified for several hours after each event. The average
423 number size distribution in LHVP and SIRTA usually had two more modes centered at 15
424 and 115 nm respectively. The summertime number distribution at GOLF was characterized
425 by two modes centered at approximately 15 and 80 nm. Unlike SIRTA and LHVP the 15
426 nm mode dominated the aerosol number distribution at GOLF.

427 During winter the contribution of particles with diameter from 10 to 30 nm to N_{10-500}
428 was almost equal to that from particles with diameters 30 to 100 nm at SIRTA (42% and
429 39%, respectively) and LHVP (44% and 40%, respectively). At GOLF the contribution of
430 particles with diameters between 10 to 30 nm increased even further (compared to
431 summer) reaching 56%, and the contribution of particles with diameters between 30 and
432 100 nm decreased to 34%. The average size distribution, shown in Fig. 8, indicates a
433 dominating mode centered below 20 nm at all sites and a smaller second mode at 60, 80,
434 and 50 nm at SIRTA, LHVP and GOLF, respectively. Similar behavior shifts of the aerosol
435 distribution to lower sizes during winter has been observed elsewhere (Bukowiecki et al.,
436 2003) where an inverse temperature dependence of the particle number concentration was
437 reported. Particles larger than 100 nm accounted for less than 20% of N_{10-500} during both
438 campaigns at all sites.

439 Taking into account the location of each site, the contribution of small particles
440 (diameters 10-30 nm) to N_{10-500} increases when moving from the SW (SIRTA) to the NE of
441 Paris (GOLF). Consequently, the contribution of particles with sizes 30-100 nm to the N_{10-}
442 $_{500}$ exhibits a decreasing (opposite) trend from the SW to the NE of Paris. Both trends were

443 observed during both seasons and indicate a persistent source of particles with diameters
444 smaller than 30 nm NE of Paris, where GOLF was located. This conclusion is further
445 supported by mobile measurements (Section 5.3) that showed that the [background](#) $N_{2.5}$ was
446 relatively stable in the area further than GOLF during summer.

450 **5.2 Impact of Paris on its surroundings**

451 To investigate the impact of the emissions from the city center on number
452 concentrations at the two satellite sites (GOLF, LHVP) the measurements were separated
453 with respect to wind direction, excluding periods when the wind speed was below 1 m s^{-1}
454 (Fig. 9). Taking into account that the area is relatively flat, it was assumed that the urban
455 center influences each of the satellite sites at certain wind directions ($215 \pm 30^\circ$ and $65 \pm 30^\circ$
456 for GOLF and SIRTA, respectively), noted with red on Fig. 9. This analysis is complicated
457 by the variability in aerosol load due to air mass origin difference. During most of the
458 summer campaign clean air masses from the Atlantic were reaching Paris (Freutel et al.,
459 2013). Air masses of different origin, which accounted for only two consequent days
460 during the summer campaign were omitted to minimize any discrepancy. During winter air
461 mass origin was more variable and a common background could not be ensured, limiting
462 this analysis only to the summer campaign.

463 During summer, the highest N_{10-500} measured at SIRTA was observed when the air
464 masses crossed the city center ($9.8 \pm 3.5 \times 10^3 \text{ cm}^{-3}$ and the lowest when the wind originated
465 from the opposite direction ($4.2 \pm 2.3 \times 10^3 \text{ cm}^{-3}$) considered later on as the background
466 concentration. The urban emissions led thus to an increase of the number concentration by
467 a factor of two at SIRTA. On the contrary, at GOLF the N_{10-500} was not clearly affected by
468 the wind direction during July 2009. N_{10-500} measurements at GOLF were higher than at
469 SIRTA, located at the same distance from Paris but on the opposite direction, by a factor of
470 three when either site was not influenced by Paris. These results do not imply that Paris did
471 not affect its surroundings during summer, but rather that the effect of the city was not
472 large enough to be observed due to higher background concentrations at the GOLF site in
473 the NE of Paris with respect to those at the SIRTA site in the SW. Mobile measurements
474 that covered mainly the N-NE area with respect to Paris support this result (see Section
475 5.3). The possibility that these observations were due to temperature changes (Bukowiecki
476 et al., 2003) was also investigated. However, no clear dependence between temperature

477 and N_{10-500} was established. As an example, at SIRTA the lowest temperatures (around 17
478 °C on average) were observed both when air masses [wherewere](#) influenced by Paris and
479 when the wind came from the opposite direction.

480 On July 21, MoLa performed stationary measurements 38 km north of Paris, which is
481 almost twice the distance of each of the stationary sites (20 km) from the city center.
482 Initially, air masses reaching MoLa were influenced by Paris emissions, based on
483 FLEXPART simulations, and $N_{2.5}$ was equal to $14.1 \times 10^3 \text{ cm}^{-3}$. However, the wind
484 direction shifted while sampling and the $N_{2.5}$ decreased by 40% reaching approximately
485 $8.5 \times 10^3 \text{ cm}^{-3}$.

486

487 **5.3 Spatial evolution of particle numbers in Paris and its surroundings**

488 The majority of mobile measurements were conducted downwind of Paris in order to
489 characterize its effect on its surroundings (von der Weiden-Reinmüller et al., 2014a;
490 2014b). These measurements were conducted in different distances from the center of
491 Paris, under various meteorological conditions, different air mass origin (marine,
492 continental) and were affected by the diurnal pattern (Fig. 7) of Paris emissions. The
493 mobile measurements were further affected by wind direction shifts which resulted in
494 monitoring of background concentrations instead of Paris emissions.

495 Paris emission measurements were identified during data analysis using FLEXPART
496 in forward mode (Section 3.4). During summer, marine air masses were predominantly
497 resulting in a relatively stable and low PM background. During winter air mass origin was
498 not as stable as during summer, yet Paris emissions were also higher, thus facilitating the
499 analysis. Variations in the number concentration due to meteorology effects or Paris
500 emissions fluctuations can be dealt with by examining short case-study periods when these
501 variables are relatively stable. However because such periods span a few hours only, the
502 measurement sample is small. If measurements throughout each campaign are considered
503 the sample size is satisfactory, yet it reflects the different conditions mentioned above. In
504 this work both approaches were considered and are presented to quantify the behavior of
505 the Paris plume downwind of the city.

506 Mobile measurements were separated, based on location, into concentric rings with
507 borders at 0.15, 0.25, 0.4, 0.6, 0.8 and 1° (16.7, 27.8, 44.4, 66.7, 88.9, and 111.1 km)
508 radius centered at kilometer zero of Paris (the official Paris center) as shown in Fig. 1. The
509 first ring includes Paris and highly populated areas surrounding it, while the second one
510 includes the greater Paris area where the two stationary sites (GOLF, SIRTA) are located.

511 During summer, when SW winds were predominant, the majority of the mobile
512 measurements took place N-NE of Paris. The $N_{2.5}$ decreased exponentially with distance
513 reaching $1.3\pm 1.6\times 10^4 \text{ cm}^{-3}$ approximately 100 km away from Paris center (Fig. 10), which
514 is not statistically different at the 95% confidence interval from the average background
515 (not influenced by Paris emissions) concentration ($1.4\pm 1.6\times 10^4 \text{ cm}^{-3}$) measured during
516 summer upwind at distances greater than 30 km from the city center by MoLa. However, at
517 distances shorter than 30 km, where GOLF is located, the background $N_{2.5}$ was almost
518 twice as large ($2.5\pm 1.1\times 10^4 \text{ cm}^{-3}$) indicating a significant regional number source affecting
519 this area. During 13 July 2009, axial measurements with respect to Paris were performed
520 under relatively stable meteorological conditions and the results, shown as black dots in
521 Fig. 10, are in good agreement with the campaign average values, following the same
522 exponential decrease. Similar behavior in that area was observed for other pollutants
523 during the same period (von der Weiden-Reinmüller et al., 2014b).

524 During winter, $N_{2.5}$ exhibited an exponential decrease with increasing distance from
525 Paris center similar to summer. However, at the center $N_{2.5}$ was 75% higher than during
526 summer. This difference was diminished in the Paris suburbs (second bar in Fig. 10),
527 reaching 20%. At distances greater than 30 km from the Paris center, no statistical
528 difference at the 95% confidence interval between $N_{2.5}$ measured during summer and
529 winter was observed. Measured $N_{2.5}$ further than 70 km away from Paris remained stable
530 ($\approx 1.4\pm 1.9\times 10^4$) and was not statistically different from the background $N_{2.5}$ concentrations
531 measured during winter ($1.1\pm 1.4\times 10^4 \text{ cm}^{-3}$) or summer ($1.4\pm 1.6\times 10^4 \text{ cm}^{-3}$). During 19
532 January 2010, axial measurements were performed and the results (shown as green
533 triangles in Fig. 10) are also in good agreement with the winter campaign averages.

534

535

536 **6. New particle formation at ground level**

537 A summary of the particle formation categorization for both campaigns can be found
538 in Fig. 11. During the summer campaign air ion bursts (of both polarities) for particles of
539 sizes between 2 and 5 nm were picked up by the AIS at [SIRTALHVP](#) on a daily basis (Fig.
540 11) with the exception of July 29. Concentrations of negatively charged particles between
541 2 and 10 nm were higher by one order of magnitude compared to positively charged. In
542 Fig. 11 we present the NPF categorization based on the negative ions which provided a
543 more sensitive way of identifying nucleation events.

544 During the summer campaign we observed 14 events at SIRTA, 14 at LHVP and 7 at
545 GOLF based on SMPS, DMPS and EAS measurements, respectively. When NPF was
546 identified at SIRTA it also took place at the city center (Fig. 11) with one exception (July
547 7). Due to technical issues of the DMPS, data for five days are not available at the LHVP
548 site. Nucleation events, if identified at two or more of the ground sites, always occurred
549 practically simultaneously (<10 min difference). N_{10-500} typically doubled at GOLF due to
550 NPF. At LHVP, an increase of N_{10-500} ranging between 50% and 150% was observed due
551 to NPF. The greatest increase in N_{10-500} , often exceeding 100%, due to NPF was observed
552 at SIRTA.

553 The highest particle growth rate (17.6 nm h⁻¹), based on SMPS measurements, was
554 observed at SIRTA on July 4 during a regional event observed at all ground sites while the
555 lowest growth rate (1.6 nm h⁻¹) was observed on July 15 at LHVP, where typically lower
556 daily growth rates compared to the two satellite sites were observed. The average growth
557 rates were 6.1 ± 1.8 nm h⁻¹, 4.6 ± 1.9 nm h⁻¹ and 5.5 ± 4.1 nm h⁻¹, at GOLF, LHVP and
558 SIRTA, respectively, during the summer campaign (Table 2). Growth rates for events that
559 occurred on all sites on the same day were 5.9 ± 2.4 nm h⁻¹, 4.5 ± 2.0 nm h⁻¹ and 8.3 ± 5.6 nm
560 h⁻¹, at GOLF, LHVP and SIRTA, respectively.

561 | During July 28 nocturnal particle formation was observed at [SIRTA](#)[LHVP](#), which
562 was identified by an increase of the ion number concentration within the 1.2–1.7 nm size
563 range. An apparent growth of cluster ions to larger diameters than the upper limit of the
564 preexisting ion pool was evident but air ions did not grow above 2 nm. Nocturnal cluster
565 growth has been observed in remote areas (Junninen et al., 2008; Kalivitis et al., 2012;
566 Hirsikko et al., 2012) and has been linked to the presence of monoterpenes (Ortega et al.,
567 2012). Sulfuric acid generation due to nighttime oxidation processes has also been
568 observed before (Mauldin et al., 2003).

569 | The CS during the summer campaign for all sites is shown in Fig. [S1S2](#) of the
570 Supplementary Information, where event and undefined days are marked with blue and
571 light blue labels, respectively. During summer the CS was half the value than in winter at
572 GOLF ($11.7 \pm 11.6 \times 10^{-3} \text{s}^{-1}$ in summer compared to $21.5 \pm 14.4 \times 10^{-3} \text{s}^{-1}$ in winter) and SIRTA
573 ($5.7 \pm 3.5 \times 10^{-3} \text{s}^{-1}$ compared to $12.3 \pm 6.8 \times 10^{-3} \text{s}^{-1}$) and 30% lower at LHVP ($12.8 \pm 7.5 \times 10^{-3} \text{s}^{-1}$
574 compared to $17.0 \pm 8.6 \times 10^{-3} \text{s}^{-1}$). During summer at SIRTA and LHVP, NPF events occurred
575 when the CS was lower than the seasonal average by 45% and 25%, respectively.
576 Undefined events at both sites were associated with CS similar to the seasonal average
577 value and non-event days with 25-30% higher CS compared to the seasonal average. In

578 winter, the high CS values in conjunction with the low solar intensity (see Section 4) most
579 likely prevented nanoparticle growth and resulted in only five events without significant
580 growth, identified only by the AIS at [SIRTALHVP](#).

581 The solar intensity influence on NPF event occurrence was evident at SIRTA and
582 LHVP. During NPF events at these two sites solar intensity was on average 30% and 20%
583 higher, respectively, compared to non-event days. At GOLF, solar intensity during non-
584 event days was found to be higher by 8% compared to actual event periods.

585 At GOLF, seven NPF events were identified, corresponding to a monthly frequency
586 of 23%. The event frequency difference between GOLF and the other two ground stations
587 was partially due to a higher frequency (23%) of undefined days (Fig. 11) caused by
588 interferences of nearby traffic. When no event was identified at all sites the CS at GOLF
589 was double ($14.7 \pm 4.5 \times 10^{-3} \text{ s}^{-1}$) compared to event days ($7.3 \pm 0.8 \times 10^{-3} \text{ s}^{-1}$), indicating that,
590 similarly to the other sites, the CS was contributing to the inhibition of NPF occurrence.
591 On several occasions (July 2, 6, 8, 23, and 28), NPF events were identified at LHVP and
592 SIRTA (on July 8 it was not clear if NPF at SIRTA occurred) but not at GOLF (Suppl. Fig.
593 [S2S3](#)). During these days CS values at GOLF were similar to event days and lower by 30%
594 compared to the campaign average, indicating that at least the CS was not suppressing
595 NPF. On two occasions (July 6 and 8) the observations show a continuous mode below 30
596 nm, either due to electrometer noise or local interferences, which prevented identification
597 of NPF. Both days were listed as non-event days but NPF may have occurred. During July
598 2, a nucleation mode was observed at LHVP for more than an hour but nucleated particles
599 did not grow above 20 nm (Class II events based on Dal Maso et al., 2005). During the
600 same time, an air ion burst between 2 and 5 nm particle diameter was picked up by the AIS
601 at [SIRTA](#) (the [same site, but at GOLF the nucleation mode was not observed. The size](#)
602 [distribution of particles above 40 nm at SIRTA](#) was not monitored), [but at GOLF the](#)
603 [nucleation mode was not observed](#). It is uncertain if nucleation occurred and ions did not
604 grow to detectable size, thus this day was listed as non-event. On July 23 NPF was
605 identified at SIRTA, but [not](#) at LHVP [only the size distribution below 40 nm was](#)
606 [monitored by AIS](#), due to technical issues. Air masses crossed SIRTA before reaching
607 GOLF and a fresh Aitken mode appeared at GOLF three hours later. Wind direction was
608 constant during that period and the lag was consistent with the time needed for an air mass
609 to travel between the two sites at the observed wind speeds (3 m s^{-1}). Similarly to July 23,
610 on July 28 an NPF event was identified at SIRTA and LHVP, while at GOLF a new Aitken
611 mode appeared after approximately three hours. From all this, it can be concluded that the

612 event frequency difference between GOLF and the other two sites can be explained to a
613 large extent by local interferences and uncertainty in identifying nucleation events.

614 Inhomogeneities with respect to the extent of NPF between locations a few tens of
615 kilometers away, similar to this work, have been reported before (Wehner et al., 2007) and
616 were attributed to cloud cover in combination with a boundary layer evolution scheme that
617 allowed such behavior. However, in the cases investigated in this work, cloud cover did
618 not appear to dictate non-event days at GOLF. Additionally, the beginning of events at all
619 sites always coincided, unlike the cases reported by Wehner et al. (2007). Despite these
620 differences, that work also noted the importance of CS in urban areas.

621

622 **7. Airborne Measurements**

623 Airborne measurements of N_{10} during summer and winter showed increased number
624 concentrations downwind of Paris accompanied by increases in light absorption measured
625 by the PSAP (Fig. 12). These results were attributed to PM emissions of Paris and are
626 referred henceforth to as the “Paris plume”. [This plume identification method assumes that](#)
627 [the only black carbon source in the area under investigation is the greater Paris region.](#)
628 [However, local sources of black carbon, such as wildfires during summer or domestic](#)
629 [heating during winter could interfere. To investigate the validity of our assumption, fire](#)
630 [maps derived from satellite information, utilizing a detection algorithm that includes small](#)
631 [fires \(Randerson et al., 2012\), were examined for the two periods \(summer and winter\)](#)
632 [under investigation. During both periods no biomass burning activity was identified ruling](#)
633 [out interferences due to this source. During winter, areas where simultaneous increases in](#)
634 [absorption and number concentration were identified and attributed to local sources and](#)
635 [not the Paris plume. The particle number concentrations in these areas were relatively low](#)
636 [though. The potential interference of these sources has a modest to small effect on our](#)
637 [estimates regarding the evolution of the Paris aerosol number plume.](#) A similar method of
638 plume identification that involves aerosol absorption was also implemented by Freney et
639 al. (2014) for the same campaign. Increased concentrations of toluene and benzene, both of
640 which are anthropogenic, were also encountered in these plumes.

641 Due to air traffic restrictions, the ATR-42 was not allowed to get closer than 30 km
642 to the Paris center, but the Paris plume could be identified as far as 200 km away from the
643 city. As stated earlier, airborne measurements were conducted on days when pollution
644 levels were above average and the flight paths were determined a priori based on
645 forecasted values of the numerical model CHIMERE, thus the sample is positively biased.

646 Mobile laboratories on the ground sampled closer to Paris during the whole campaign, but
647 separating the plume from the background was cumbersome (von der Weiden-Reinmüller
648 et al., 2014a).

649 During summer the averaged aircraft measured N_{10} within the Paris plume was
650 $10.1 \pm 5.6 \times 10^3 \text{ cm}^{-3}$, which was 14% higher than the concentrations observed outside of the
651 Paris plume ($8.8 \pm 6.5 \times 10^3 \text{ cm}^{-3}$), defining the background concentrations. The high
652 background number concentrations in this N to E quadrant where all of the summer flights
653 but one took place (grey, blue and green lines in Fig. 2) are consistent with the ground
654 (stationary and mobile) observations.

655 During all summer flights, with the exception of July 25, “hot spots” outside of the
656 Paris plume where particle number concentrations similar to or higher than those of the
657 Paris plume were identified without increase in black carbon or anthropogenic volatile
658 organic compounds (VOCs; benzene, toluene). The “hot spots” where the particle number
659 increase occurred were separated into three groups based on their location with respect to
660 the Paris plume as “upwind”, “alongside” and “local”.

661 The “upwind” events were identified upwind of Paris four times, always near IDF
662 (Fig. 12b) and simultaneously with regional nucleation events observed at least at two of
663 the ground sites. The number concentration increases were thus attributed to NPF.
664 Assessment of the spatial extension of these events was complicated by the presence of the
665 plume and limited by the designated flight paths (Fig. 2). In general, the N_{10} measured
666 upwind was 40% higher than that measured in the plume during these “upwind” NPF
667 events.

668 The “alongside” events occurred at an average distance of 40 km from the plume
669 edge and were attributed to NPF (Fig. 12d). The average number concentration increased
670 by 47% in comparison to the concentration within the Paris plume. The area in between the
671 Paris plume and the hot spot area always exhibited at least 20% lower concentrations than
672 the latter two (Fig. 12d shows the number concentration with respect to cardinal
673 coordinates and Suppl. Fig. 34 as a time-series). The alongside events occurred during four
674 flights (July 1, 15, 21, and 28), two of which were non-event days for all ground sites and
675 two when NPF was identified at SIRTa and LHVP, but not at GOLF. The high N_{10} areas
676 covered approximately $3,000 \text{ km}^2$ along the plume.

677 In order to investigate why the alongside events occurred only on one side of the
678 Paris plume during these flights, each flight path was separated into three areas: (1) the
679 area with high N_{10} outside of the plume, (2) the plume area and (3) the area on the other

680 side of the plume, where no increase in particle number was observed. The observed
681 differences between both sides of the Paris plume with respect to the CS, solar intensity
682 and isoprene concentration, which has been reported as a potential inhibitor of NPF in
683 forested areas (Kiendler-Scharr et al., 2009; Kanawade et al., 2011), were 12%, 5% and
684 6%, respectively (Suppl. Fig. 45). These relatively small differences probably cannot
685 explain the observed [phenomenon](#). Other pollutants such as benzene,
686 toluene, monoterpenes, methacrolein, methyl vinyl ketone, O₃, CO, but also meteorological
687 parameters such as temperature and RH were investigated in order to identify potential
688 reasons for the different particle number concentrations between both sides of the plume.
689 Differences in all the investigated parameters were less than 10%. These events clearly
690 require more investigation with instrumentation that can sample particles smaller than 10
691 nm in combination with trace gas measurements relevant to NPF (e.g. SO₂). [Unfortunately,](#)
692 [there were no ground measurements in the areas in which the alongside events were](#)
693 [identified.](#)

694 The “local” events were the most frequent (6 out of the 11 study cases) and occurred
695 either at the north coast of France downwind of the city of Fecamp (4 events) and were
696 associated with high or medium tide height (indicating influence of ship emissions?), or
697 near the city of Aulnoye-Aymeries (4 events). On two occasions these events were
698 identified on both locations during the same flight. Because the local events were always
699 associated with specific areas, the particle number concentration increase was attributed to
700 local sources.

701 During the three winter flights, the Paris plume $N_{2.5}$ was 45% higher than the
702 background and no “hot spots” were identified, consistent with ground measurements
703 where no NPF was identified.

704

705 **8. Summary and conclusions**

706 Ambient aerosol number concentrations were monitored at the center of Paris
707 (LHVP) along with two satellite suburban stations (SIRTA, SW and GOLF, NE). Mobile
708 measurements were performed by two mobile laboratories and the SAFIRE aircrafts during
709 July 2009 (summer, ATR-42) and January - February 2010 (winter, Piper-Aztec).

710 During summer, N_{10-500} (number concentration for particles between 10 and 500 nm
711 diameter) at the city center was lower by 14% than at the downwind (GOLF) and 54%
712 higher than at the upwind (SIRTA) suburban site, respectively. The contribution of
713 particles with diameters between 10 and 30 nm to N_{10-500} increased from the mostly upwind

714 suburban site (30% at SIRTA) over the city center (40% at LHVP) to the mostly
715 downwind suburban site (50% at GOLF). The contribution of particles with diameters
716 between 30 and 100 nm ranged between 40-50% and followed the opposite trend (highest
717 upwind, lowest downwind).

718 During summer at SIRTA, N_{10-500} increased to $9.9 \pm 2.4 \times 10^3 \text{ cm}^{-3}$ when the site was
719 downwind of Paris and decreased to $4.2 \pm 2.5 \times 10^3 \text{ cm}^{-3}$ when the site was upwind. At
720 GOLF, located at approximately the same distance from the city center as SIRTA but in
721 the opposite direction (NE), the effect of Paris emissions was not clear, suggesting a high
722 background N_{10-500} at the measurement location for all wind directions.

723 NPF events were observed at all sites during summer. At SIRTA and LHVP, events
724 were identified every second day and at GOLF once every four days on average. The lower
725 frequency of NPF events at GOLF was mainly due to interferences from nearby traffic and
726 instrumental limitations which did not allow clear event identification. NPF occurred
727 during periods when the CS was lower by 45%, 25% and 50% at SIRTA, LHVP and
728 GOLF, respectively, in comparison to each site's average value, indicating that the CS may
729 have been a controlling factor for the frequency of events. Solar intensity was higher by
730 30% and 20% on event days compared to non-event days at SIRTA and LHVP,
731 respectively. At GOLF, solar intensity was higher by 8% during non-event days compared
732 to event days. On average, NPF events caused N_{10-500} to double at all stationary
733 measurement sites.

734 Average particle growth rates were 5.5, 4.6 and 6.1 nm h^{-1} at SIRTA, LHVP and
735 GOLF, respectively. The differences between these average growth rates were not
736 statistically significant.

737 The particle number concentration within the Paris emission plume was found to
738 decrease exponentially on the ground with distance from the Paris center during both
739 campaigns. At distances from the city center greater than 70 km, $N_{2.5}$ was approximately
740 $1.4 \times 10^4 \text{ cm}^{-3}$ regardless of season or whether the measurements were affected by the Paris
741 plume. However during summer background conditions (not affected by Paris), $N_{2.5}$ close
742 to GOLF (second circle in Fig. 1) was approximately a factor of two higher, in agreement
743 with N_{10-500} measurements at GOLF that indicated a higher background in the region NE of
744 Paris.

745 The Paris plume was identified by aircraft measurements at an altitude of 600 m,
746 using black carbon as a tracer, as far as 200 km away from the city center. Averaged N_{10}
747 outside and within the Paris plume were $8.8 \pm 6.5 \times 10^3$ and $10.1 \pm 5.6 \times 10^3 \text{ cm}^{-3}$, respectively

748 which corresponds to a 33% increase. During summer, “hot spots” of high particle number
749 concentrations were identified outside of the Paris plume at 600 m altitude. On four
750 occasions the particle number concentration increase was located upwind of the ground
751 stations simultaneously with regional NPF observed on the ground at least at two of the
752 sites. These increases therefore were attributed to NPF. Increased particle number
753 concentrations were also identified along one side of the plume on four occasions. A
754 number of parameters were investigated including CS, solar irradiance, anthropogenic and
755 biogenic VOC concentrations among others, as possible explanations for this asymmetry.
756 All differences observed between both sides of the Paris plume were approximately 10%
757 or lower, so none of these could explain the observations.

758 During winter the absolute N_{10-500} was higher by a factor of two at both suburban
759 sites and by 36% at the city center compared to summer. At LHVP particles from 10 to 30
760 nm accounted for 44% of the N_{10-500} on average and those from 30 to 100 nm for 40%. At
761 GOLF, similar to summer, the N_{10-500} was dominated by particles with diameters between
762 10 and 30 nm which accounted for 56%, followed by particles from 30 to 100 nm (33%),
763 following the same trends as during summer. At SIRTAs the contribution of particles from
764 10 to 30 nm and from 30 to 100 nm to the N_{10-500} was 42% and 39%, respectively.
765 Regardless of site or season a mode, centered at a diameter below 20 nm, was always
766 present and was dominating during winter at all sites. During winter the higher CS and
767 lower solar intensity compared to summer prevented particles from growing to sizes larger
768 than 10 nm.

769 A complete year of air ion measurements (including the two intensive campaigns
770 discussed in the present paper) has been recently presented by Dos Santos et al. (2015).
771 These measurements took place in the MEGAPOLI site in the center of Paris (LHVP
772 station) from July 2009 to September 2010. During this year, the highest NPF frequency in
773 Paris was observed during July 2009 (the summer campaign examined in this work) and
774 the lowest during the winter (which includes the winter campaign in this work). Therefore
775 our analysis above focused on two extreme NPF periods in Paris. During summer under
776 clean conditions and peak NPF frequency and during winter under polluted conditions and
777 minimal NPF frequency.

778
779
780 **Acknowledgements.** Parts of the research leading to these results have received funding
781 from the European Union’s Seventh Framework Programme FP7 within the project

782 MEGAPOLI, grant agreement no. 212520 and the FP7 IDEAS project ATMOPACS. The
783 research conducted by MPIC was supported by internal funds. Support from the French
784 ANR project MEGAPOLI – PARIS (ANR-09-BLAN-0356) and from the CNRS-
785 INSU/FEFE via l’ADEME (n° 0962c0018) is acknowledged. We are grateful for the
786 logistical support in the field by IPSL/SIRTA, by Laboratoire d’Hygiène de la Ville de
787 Paris (LHVP) and by the staff of the Golf Départemental de la Poudrerie. The SAFIRE
788 team is acknowledged and thanked for performing ATR-42 flights and measurements.

789

790

791

792

793

794

795

796

797

798

799

800 9. References

801 Aalto, P. P., Hämeri, K., Becker, E., Weber, R., Salm, J., Mäkelä, J.M., Hoell, C.,
802 O’Dowd, C.D., Karlsson, H., Hansson, H.-C., Väkevä, M., Koponen, I.K., Buzorius, [G.](#)
803 and [G.](#) Kulmala, M.: Physical characterization of aerosol particles during nucleation
804 events, *Tellus*, 53B, 344-358, 2001.

805 Alam, A., Shi, J. P. and Harrison, R. M.: Observations of new particle formation in urban
806 air, *J. Geophys. Res.*, 108, 4093, doi:10.1029/2001JD001417, 2003.

807 Baklanov, A., Lawrence, M., Pandis, S., Mahura, A., Finardi, S., Moussiopoulos, N.,
808 Beekmann, M., Laj, P., Gomes, L., Jaffrezo, J.-L., Borbon, A., Coll, I., Gros, V.,
809 Sciare, J., Kukkonen, J., Galmarini, S., Giorgi, F., Grimmond, S., Esau, I., Stohl, A.,
810 Denby, B., Wagner, T., Butler, T., Baltensperger, U., Builtjes, P., van den Hout, D.,
811 van der Gon, H. D., Collins, B., Schluenzen, H., Kulmala, M., Zilitinkevich, S.,
812 Sokhi, R., Friedrich, R., Theloke, J., Kummer, U., Jalkanen, L., Halenka, T.,
813 Wiedensholer, A., Pyle, J., and Rossow, W. B.: MEGAPOLI: concept of multi-scale
814 modelling of megacity impact on air quality and climate, *Adv. Sci. Res.*, 4, 115-120,
815 doi:10.5194/asr-4-115-2010, 2010.

816 Baltensperger, U., Streit, N., Weingartner, E., Nyeki, S., [PrevotPrévôt](#), A. S. H., Van
817 Dingenen, R., Virkkula, A., Putaud, J. P., Even, A., Brink, H., Blatter, A., Nefstel, A.,
818 and Gaggeler, H. W.: Urban and rural aerosol characterization of summer smog events
819 during the PIPAPO field campaign in Milan, Italy, *J. Geophys. Res.-Atmos.*, 107, 8193,
820 10.1029/2001JD001292, 2002.

821 [Beekmann, M., Prévôt, A. S. H., Drewnick, F., Sciare, J., Pandis, S. N.,](#)
822 [Denier van der Gon, H. A. C., Crippa, M., Freutel, F., Poulain, L., Ghersi, V.,](#)
823 [Rodriguez, E., Beirle, S., Zotter, P., von der Weiden-Reinmüller, S.-L., Bressi, M.,](#)
824 [Fountoukis, C., Petetin, H., Szidat, S., Schneider, J., Rosso, A., El Haddad, I.,](#)
825 [Megaritis, A., Zhang, Q. J., Michoud, V., Slowik, J. G., Moukhtar, S., Kolmonen, P.,](#)
826 [Stohl, A., Eckhardt, S., Borbon, A., Gros, V., Marchand, N., Jaffrezo, J. L.,](#)
827 [Schwarzenboeck, A., Colomb, A., Wiedensohler, A., Borrmann, S., Lawrence, M.,](#)
828 [Baklanov, A., and Baltensperger, U.: In-situ, satellite measurement and model evidence](#)
829 [for a dominant regional contribution to fine particulate matter levels in the Paris](#)
830 [Megacity, Atmos. Chem. Phys. Discuss., 15, 8647-8686, doi:10.5194/acpd-15-8647-](#)
831 [2015, 2015.](#)

832 [Bermúdez, V., Luján, J., Ruiz, S., Campos, D. and Linares, W.: New European driving](#)
833 [cycle assessment by means of particle size distributions in a light-duty diesel engine](#)
834 [fuelled with different fuel formulations, Fuel, 140, 649659,](#)
835 [doi:10.1016/j.fuel.2014.10.016, 2015.](#)

836 Barbone, F., Bovenzi, M., Cavallieri, F. and Stanta, G.: Air pollution and lung cancer in
837 Trieste, Italy, Am. J. Epidemiol., 141, 1161-1169, 1995.

838 Beeson, W. L., Abbey, D.E. and Knutsen, S.F.: Long term concentrations of ambient air
839 pollutants and incident lung cancer in California adults: results from the ASMOGH
840 study, Environ. Health. Perspect. 106, 813-822, 1998.

841 Birmili, W., Stratmann, F., and Wiedensohler, A.: Design of a DMA-based size
842 spectrometer for a large particle size range and stable operation, J. Aerosol Sci., 30,
843 549–553, doi:10.1016/S0021-8502(98)00047-0, 1999.

844 Birmili, W. and Wiedensohler, A.: New particle formation in the continental boundary
845 layer: meteorological and gas phase parameter influence. Geophys. Res. Lett., 27,
846 3325–3328, 2000.

847 Bukowiecki, N., Dommen, J., [PrevotPrévôt](#), A. S. H., Richter, R., Weingartner, E., and
848 Baltensperger, U.: A mobile pollutant measurement laboratory - measuring gas phase
849 and aerosol ambient concentrations with high spatial and temporal resolution, Atmos.
850 Environ., 36, 5569–5579, 2002.

851 Bukowiecki, N., Dommen, J., Prévôt, A. S. H., Weingartner, E., and Baltensperger, U.:
852 Fine and ultrafine particles in the Zürich (Switzerland) area measured with a mobile
853 laboratory: an assessment of the seasonal and regional variation throughout a year,
854 Atmos. Chem. Phys., 3, 1477-1494, doi:10.5194/acp-3-1477-2003, 2003.

855 [Bukowiecki, N., Hill, M., Gehrig, R., Zwicky, C., Lienemann, P., Hegedüs, F., Falkenberg,](#)
856 [G., Weingartner, E. and Baltensperger, U.: Trace metals in ambient air: Hourly size-](#)
857 [segregated mass concentrations determined by Synchrotron-XRF, Environ. Sci.](#)
858 [Technol., 39, 5754-5762, doi:10.1021/es048089m, 2005.](#)

859 Carslaw, K. S., Clegg, S. L., and Brimblecombe, P.: A thermodynamic model of the
860 system HCl-HNO₃-H₂SO₄-H₂O, including solubilities of HBr, from <200 K to 328 K, J.
861 Phys. Chem., 99, 11557–11574, 1995.

862 [Chan, T. and Mozurkewich, M.: Application of absolute principal component analysis to](#)
863 [size distribution data: identification of particle origins, Atmos. Chem. Phys., 7, 887–](#)
864 [897, doi:10.5194/acp-7-887-2007, 2007.](#)

865 Chung, C. E., Ramanathan, V., Kim, D., and Podgorny, I.: Global anthropogenic aerosol
866 direct forcing derived from satellite and ground-based observations, J. Geophys. Res.,
867 110, D24207, doi:10.1029/2005JD006356, 2005.

868 Clegg, S., Brimblecombe, L., P. and Wexler, A. S.: A thermodynamic model of the system
869 H⁺-NH₄⁺-SO₄²⁻-NO₃⁻-H₂O at tropospheric temperatures, J. Phys. Chem., A102, 2137–
870 2154, doi:10.1021/jp973043j, 1998.

871 | [Couvidat, F., Kim, Y., Sartelet, K., Seigneur, C., Marchand, N., and Sciare, J. : Modeling](#)
872 | [secondary organic aerosol in an urban area: Application to Paris, France, *Atmos. Chem.*](#)
873 | [Phys., 13, 983-996, 2013.](#)

874 | Crippa, M., P.F. DeCarlo, J.G. Slowik, C. Mohr, M.F. Heringa, R. Chirico, L. Poulain, F.
875 | Freutel, J. Sciare, J. Cozic, C.F. Di Marco, M. Elsasser, J.B. Nicolas, N. Marchand, E.
876 | Abidi, A. Wiedensohler, F. Drewnick, J. Schneider, S. Borrmann, E. Nemitz, R.
877 | Zimmermann, J.L. Jaffrezo, A.S.H. Prévôt, U. Baltensperger, Wintertime aerosol
878 | chemical composition and source apportionment of the organic fraction in the
879 | metropolitan area of Paris, *Atmos. Chem. Phys.*, 13, 961-981, 2013a.

880 | Crippa, M., Canonaco, F., Slowik, J. G., El Haddad, I., DeCarlo, P. F., Mohr, C., Heringa,
881 | M., Chirico, R., Marchand, N., Temime, B., Poulain, L., Baltensperger, U., and Prévôt,
882 | A. S. H.: Primary and secondary organic aerosols origin by combined gas-particle phase
883 | source apportionment, *Atmos. Chem. Phys.*, 13, 8411-8426, 2013b.

884 | Crumeyrolle S., H.E. Manninen, A. Schwarzenboeck, L. Gomes, G. Roberts, M. Kulmala,
885 | K. Sellegri, P. Laj. New particle formation events measured by the ATR-42 during the
886 | EUCAARI campaign. *Atmos. Chem. Phys.*, 10, 6721-6735, 2010.

887 | Dal Maso, M., Kulmala, M., Lehtinen, K., Mäkelä, J., Aalto, P. and O'Dowd, C.:
888 | Condensation and coagulation sinks and formation of nucleation mode particles in
889 | coastal and boreal forest boundary layers, *J. Geophys. Res.: Atmospheres*, 107(D19),
890 | [PAR 2-1-PAR 2-10](#), doi:10.1029/2001JD001053, 2002.

891 | Dal Maso, M., Kulmala, M., Riipinen, I., Wagner, R., Hussein, T., Aalto, P., and Lehtinen,
892 | K. E. J.: Formation and growth of fresh atmospheric aerosols: Eight years of aerosol
893 | size distribution data from SMEAR II, Hyytiälä, Finland, *Boreal Environ. Res.*, 10,
894 | 323-336, 2005.

895 | [Dos Santos, V. N., Herrmann, E., Manninen, H. E., Hussein, T., Hakala, J., Nieminen, T.,](#)
896 | [Aalto, P. P., Merkel, M., Wiedensohler, A., Kulmala, M., Petäjä, T., and Hämeri, K.:](#)
897 | [Variability of air ion concentrations in urban Paris, *Atmos. Chem. Phys. Discuss.*, 15,](#)
898 | [10629-10676, doi:10.5194/acpd-15-10629-2015, 2015.](#)

899 | Drewnick, F., Böttger, T., von der Weiden-Reinmüller, S.-L., Zorn, S. R., Klimach, T.,
900 | Schneider, J., and Borrmann, S.: Design of a mobile aerosol research laboratory and
901 | data processing tools for effective stationary and mobile field measurements, *Atmos.*
902 | *Meas. Tech.*, 5, 1443-1457, doi:10.5194/amt-5-1443-2012, 2012.

903 | Dunn, M.J., Jimenez, J.L., Baumgardner, D., Castro, T., McMurry, P.H., Smith, J.N.:
904 | Measurements of Mexico City nanoparticle size distributions: observations of new
905 | particle formation and growth. *Geophys. Res. Lett.*, 31, L10102,
906 | doi:10.1029/2004GL019483, 2004.

907 | Engelhart, G. J., Hildebrandt, L., Kostenidou, E., Mihalopoulos, N., Donahue, N. M., and
908 | Pandis, S. N.: Water content of aged aerosol, *Atmos. Chem. Phys.*, 11, 911-920,
909 | doi:10.5194/acp-11-911-2011, 2011.

910 | Favez, O., Cachier, H., Sciare, J., Le Moullec, Y.: Characterization and contribution to
911 | PM_{2.5} of semi-volatile aerosols in Paris (France), *Atmos. Environ.*, 41, 7969-7976, 2007.

912 | Freney, E. J., Sellegri, K., Canonaco, F., Colomb, A., Borbon, A., Michoud, V.,
913 | Doussin, J.-F., Crumeyrolle, S., Amarouche, N., Pichon, J.-M., Bourianne, T.,
914 | Gomes, L., [PrevotPrévôt](#), A. S. H., Beekmann, M., and Schwarzenböeck, A.:
915 | Characterizing the impact of urban emissions on regional aerosol particles: airborne
916 | measurements during the MEGAPOLI experiment, *Atmos. Chem. Phys.*, 14, 1397-
917 | 1412, 2014.

918 | Freutel, F., Schneider, J., Drewnick, F., von der Weiden-Reinmüller, S.-L., Crippa, M.,
919 | Prévôt, A. S. H., Baltensperger, U., Poulain, L., Wiedensohler, A., Sciare, J., Sarda-
920 | Estève, R., Burkhardt, J. F., Eckhardt, S., Stohl, A., Gros, V., Colomb, A., Michoud, V.,

921 Doussin, J. F., Borbon, A., Haeffelin, M., Morille, Y., Beekmann, M., and
 922 Borrmann, S.: Aerosol particle measurements at three stationary sites in the megacity of
 923 Paris during summer 2009: meteorology and air mass origin dominate aerosol particle
 924 composition and size distribution, *Atmos. Chem. Phys.*, 13, 933-959, 2013.

925 [Fuchs, N., and A. Sutugin, Highly dispersed aerosol, in Topics in Current Aerosol](#)
 926 [Research, edited by G. Hidy, and J. Brock, Pergamon, New York, 1971.](#)

927 Gurjar, B. R., Butler, T. M., Lawrence, M. G., and Lelieveld, J.: Evaluation of emissions
 928 and air quality in megacities, *Atmos. Environ.*, 42, 1593–1606, 2008.

929 Hering, S. V., Kreisberg, N. M., Stolzenburg, M. R., and Lewis, G. S.: Comparison of
 930 particle size distributions at urban and agricultural sites in California's San Joaquin
 931 Valley, *Aerosol Sci. Technol.*, 41, 86-96, 2007.

932 Hirsikko, A., Laakso, L., Hörrak, U., Aalto, P., Kerminen, V.-M., and Kulmala, M.:
 933 Annual and size dependent variation of growth rates and ion concentrations in boreal
 934 forest, *Boreal Environ. Res.*, 10, 357–369, 2005.

935 Hirsikko, A., Bergman, T., Laakso, L., Dal Maso, M., Riipinen, I., Hörrak, U., and
 936 Kulmala, M.: Identification and classification of the formation of intermediate ions
 937 measured in boreal forest, *Atmos. Chem. Phys.*, 7, 201–210, 2007.

938 Hirsikko, A., Vakkari, V., Tiitta, P., Manninen, H. E., Gagné, S., Laakso, H., Kulmala, M.,
 939 Mirme, A., Mirme, S., Mabaso, D., Beukes, J. P., and Laakso, L.: Characterisation of
 940 sub-micron particle number concentrations and formation events in the western
 941 Bushveld Igneous Complex, South Africa, *Atmos. Chem. Phys.*, 12, 3951-3967, 2012.

942 [Hussein, T., Puustinen, A., Aalto, P., Mäkelä, J., Hämeri, K. and Kulmala, M.: Urban](#)
 943 [aerosol number size distributions, *Atmos. Chem. Phys.*, 4, 391–411, doi:10.5194/acp-4-](#)
 944 [391-2004, 2004.](#)

945 IPCC 2007 *Fourth Assessment Report (IPCC AR4)* (Geneva: Intergovernmental Panel on
 946 Climate Change), 2007.

947 Jayne, J.T., Leard, D.C., Zhang, X., Davidovits, P., Smith, K. A., Kolb, C. E., and
 948 Worsnop, D. R.: Development of an aerosol mass spectrometer for size and composition
 949 analysis of submicron particles, *Aerosol Sci. Technol.*, 33, 49–70, 2000.

950 Jimenez, J. L., Jayne, J. T., Shi, Q., Kolb, C. E., Worsnop, D. R., Yourshaw, I., Seinfeld, J.
 951 H., Flagan, R. C., Zhang, X., Smith, K. A., Morris, J., and Davidovits, P.: Ambient
 952 aerosol sampling using the Aerodyne Aerosol Mass Spectrometer, *J. Geophys. Res.*,
 953 108, 8425, doi:10.1029/2001JD001213, 2003.

954 Junninen, H., Hulkkonen, M., Riipinen, I., Nieminen, T., Hirsikko, A., Suni, T., Boy, M.,
 955 Lee, S.-H., Vana, M., Tammet, H., Kerminen, V.-M., and Kulmala, M.: Observations
 956 on nocturnal growth of atmospheric clusters, *Tellus*, 60B, 365–371, 2008.

957 Kalivitis N., I. Stavroulas, A. Bougiatioti, G. Kouvarakis, S. Gagne, H. E. Manninen, M.
 958 Kulmala, and Mihalopoulos, N.: Night-time enhanced atmospheric ion concentrations in
 959 the marine boundary layer, *Atmos. Chem. Phys.*, 12, 3627–3638, 2012.

960 Kanawade, V. P., B. T. Jobson, A. B. Guenther, M. E. Erupe, S. N. Pressley, S. N.
 961 Tripathi, and Lee, S.-H.: Isoprene suppression of new particle formation in a mixed
 962 deciduous forest, *Atmos. Chem. Phys.*, 11, 6013–6027, 2011.

963 Kiendler-Scharr, A., Wildt, J., Dal Maso, M., Hohaus, T., Kleist, E., Mente, T. F.,
 964 Tillmann, R., Uerlings, R., Schurr, U., and Wah-ner, A.: New particle formation in
 965 forests inhibited by isoprene emissions, *Nature*, 461, 381–384, 2009.

966 Komppula, M., Sihto, S.-L., Korhonen, H., Lihavainen, H., Kerminen, V.-M.,
 967 Kulmala, M., and Viisanen, Y.: New particle formation in air mass transported between
 968 two measurement sites in Northern Finland, *Atmos. Chem. Phys.*, 6, 2811-2824, 2006.

969 Kulmala, M., Dal Maso, M., Mäkelä, J., Pirjola, L., Väkevä, M., Aalto, P., Miikkulainen,
 970 P., Hämeri, K. and O'Dowd, C.: On the formation, growth and composition of

971 nucleation mode particles, *Tellus B*, 53(4), 479–490, [doi:10.1034/j.1600-](https://doi.org/10.1034/j.1600-0889.2001.530411.x)
972 [0889.2001.530411](https://doi.org/10.1034/j.1600-0889.2001.530411.x), [doi:10.1034/j.1600-0889.2001.530411.x](https://doi.org/10.1034/j.1600-0889.2001.530411.x), 2001.

973 Kulmala, M., Vehkamäki, H., Petaja, T., Dal Maso, M., Lauri, A., Kerminen, V. M.,
974 Birmili, W., and McMurry, P. H.: Formation and growth rates of ultrafine atmospheric
975 particles: a review of observations, *J. Aerosol Sci.*, 35, 143–176, 2004.

976 Laakso, L., Hussein, T., Aarnio, P., Komppula, M., Hiltunen, V., Viisanen, Y., and
977 Kulmala, M.: Diurnal and annual characteristics of particle mass and number
978 concentrations in urban, rural and arctic environments in Finland, *Atmos. Environ.* 37,
979 2629–2641, 2003.

980 Laden, F., Schwartz, J., Speizer, F. E., and Dockery, D.: [AirReduction in fine particulate](https://doi.org/10.1164/rccm.200503-443OC)
981 [air](https://doi.org/10.1164/rccm.200503-443OC) pollution and mortality: [a continued follow-up in Extended followup of the Harvard](https://doi.org/10.1164/rccm.200503-443OC)
982 [Six Cities study, *Epidemiology*, 12, S81, 2001](https://doi.org/10.1164/rccm.200503-443OC) Study, *Am. J. Respir. Crit. Care Med.*,
983 [173, 667–672](https://doi.org/10.1164/rccm.200503-443OC), [doi:10.1164/rccm.200503-443OC](https://doi.org/10.1164/rccm.200503-443OC), 2006.

984 Lawrence, M. G., Butler, T. M., Steinkamp, J., Gurjar, B. R., and Lelieveld, J.: Regional
985 pollution potentials of megacities and other major population centers, *Atmos. Chem.*
986 *Phys.*, 7, 3969–3987, 2007.

987 Lohmann U. and Feichter J.: Global indirect aerosol effects: a review, *Atmos. Chem.*
988 *Phys.*, 5, 715–737, 2005.

989 Manninen, H. E., Nieminen, T., Asmi, A., et al.: EUCAARI ion spectrometer
990 measurements at 12 European sites – analysis of new-particle formation events, *Atmos.*
991 *Chem. Phys.* 10, 7907–7927, 2010.

992 Massucci, M., Clegg, S. L., and Brimblecombe, P.: Equilibrium partial pressures,
993 thermodynamic properties of aqueous and solid phases, and Cl₂ production from
994 aqueous HCl and HNO₃ and their mixtures, *J. Phys. Chem. A*, 103, 4209–4226, 1999.

995 [Mauldin, R., Cantrell, C., Zondlo, M., Kosciuch, E., Eisele, F., Chen, G., Davis, D.,](https://doi.org/10.1029/2003JD003410)
996 [Weber, R., Crawford, J., Blake, D., Bandy, A. and Thornton, D.: Highlights of OH,](https://doi.org/10.1029/2003JD003410)
997 [H₂SO₄, and methane sulfonic acid measurements made aboard the NASA P-3B during](https://doi.org/10.1029/2003JD003410)
998 [Transport and Chemical Evolution over the Pacific, *J. Geophys. Res.*, 108, 8796–8808,](https://doi.org/10.1029/2003JD003410)
999 [doi:10.1029/2003JD003410](https://doi.org/10.1029/2003JD003410), 2003.

1000 [McNaughton, C. S., Clarke, A. D., Howell, S. G., Pinkerton, M., Anderson, B., and](https://doi.org/10.1080/02786820601118406)
1001 [Thornhill, L.: Results from the DC-8 Inlet Characterization Experiment \(DICE\):](https://doi.org/10.1080/02786820601118406)
1002 [Airborne versus surface sampling of mineral dust and sea salt aerosols. *Aerosol Sci.*](https://doi.org/10.1080/02786820601118406)
1003 [*Technol.*, 41, 136–159, doi:10.1080/02786820601118406](https://doi.org/10.1080/02786820601118406), 2007.

1004 Menut L. and Bessagnet, B.: Atmospheric composition forecasting in Europe, *Annales*
1005 *Geophysicae*, 28, 61-74, 2010.

1006 Menut L, Bessagnet, B., Khvorostyanov, D., Beekmann, M., Blond, N., Colette, A., Coll,
1007 I., Curci, G., Foret, G., Hodzic, A., Mailler, S., Meleux, F., Monge, J.L., Pison, I., Siour,
1008 G., Turquety, S., Valari, M., Vautard, R. and Vivanco, M.G.: CHIMERE 2013: a model
1009 for regional atmospheric composition modelling, *Geoscientific Model Development*, 6,
1010 981-1028, 2013.

1011 [Michoud, V., Kukui, A., M. Camredon, A. Colomb, A. Borbon, K. Miet, B. Aumont,](https://doi.org/10.5194/acp-12-11951-2012)
1012 [M. Beekmann, R. Durand-Jolibois, S. Perrier, P. Zapf, G. Siour, W. Ait-Helal,](https://doi.org/10.5194/acp-12-11951-2012)
1013 [N. Locoge, S. Sauvage, C. Afif, V. Gros, M. Furger, G. Ancellet, and J. F. Doussin:](https://doi.org/10.5194/acp-12-11951-2012)
1014 [Radical budget analysis in a suburban European site during the MEGAPOLI summer](https://doi.org/10.5194/acp-12-11951-2012)
1015 [field campaign, *Atmos. Chem. Phys.*, 12, 11951-11974, 2012.](https://doi.org/10.5194/acp-12-11951-2012)

1016 Molina, M. J. and Molina, L. T.: Critical Review: Megacities and atmospheric pollution, *J.*
1017 *Air Waste Manage. Assoc.*, 54, 644–680, 2004.

1018 [Molina, L. T., Molina, M. J., Slott, R., Kolb, C. E., Gbor, P. K., Meng, F., Singh, R.,](https://doi.org/10.1080/02786820601118406)
1019 [Galvez, O., Sloan, J. J., Anderson, W., Tang, X. Y., Shao, M., Zhu, T., Zhang, Y. H.,](https://doi.org/10.1080/02786820601118406)
1020 [Hu, M., Gur-jar, B. R., Artaxo, P., Oyola, P., Gramsch, E., Hidalgo, P., and Gertler A.:](https://doi.org/10.1080/02786820601118406)

1021 | [Critical Review Supplement: Air quality in selected Megacities, J. Air Waste Manage.](#)
1022 | [Assoc. 12, 1–73, doi:10.1080/10473289.2004.1047101, 2004.](#)

1023 | McMurry, P. H., Woo, K. S., Weber, R., Chen, D.-R., and Pui, D. Y. H.: Size
1024 | Distributions of 3 to 10 nm Atmospheric Particles: Implications for nucleation
1025 | mechanisms, [Philosophical Transactions of the Royal Society, London, T. Roy. Soc.](#)
1026 | [Lond. A, 358, 2625–2642, 2000.](#)

1027 | McMurry, P. H., [et al Fink, M., Sakuri, H., Stolzenburg, M., Mauldin III, R. L., Smith, J.,](#)
1028 | [Eisele, F. L., Moore, K., Sjostedt, S., Tanner, D., Huey, L.G., Nowak, J. B., Edgerton,](#)
1029 | [E., and Voisin, D.:](#) A criterion for new particle formation in the sulfur-rich Atlanta
1030 | atmosphere, *J. Geophys. Res.*, 110, D22S02, [doi:10.1029/2005JD005901,](#)
1031 | [doi:10.1029/2005JD005901, 2005.](#)

1032 | Mirme, A., Tamm, E., Mordas, G., Vana, M., Uin, J., Mirme, S., Bernotas, T., Laakso, L.,
1033 | Hirsikko, A., and Kulmala, M.: A wide-range multi-channel Air Ion Spectrometer,
1034 | *Boreal Environ. Res.*, 12, 247–264, 2007.

1035 | Nafstad, P., Haheim, L.L., Oftedal, B., Gram, F., Holme, I., Hjermmann, I. and Leren, P.:
1036 | Lung cancer and air pollution: a 27 years follow-up of 16 209 Norwegian men, *Thorax*,
1037 | 58, 1071-1076, 2003.

1038 | Nyberg, F., Gustavsson, P., Järup, L., Bellander, T., Berglind, N., Jakobsson, R. and
1039 | Pershagen, G.: Urban air pollution and lung cancer in Stockholm, *Epidemiology*, 11,
1040 | 487-495, 2000.

1041 | [Organization for Economic Co-operation and Development:](#) Definition of Functional
1042 | Urban Areas (FUA) for the OECD metropolitan database, [http://www.oecd.org/gov/regional-](http://www.oecd.org/gov/regional-policy/Definition-of-Functional-Urban-Areas-for-the-OECD-metropolitan-database.pdf)
1043 | [policy/Definition-of-Functional-Urban-Areas-for-the-OECD-metropolitan-database.pdf](http://www.oecd.org/gov/regional-policy/Definition-of-Functional-Urban-Areas-for-the-OECD-metropolitan-database.pdf) available at:
1044 | [http://www.oecd.org/gov/regional-policy/Definition-of-Functional-Urban-Areas-for-](http://www.oecd.org/gov/regional-policy/Definition-of-Functional-Urban-Areas-for-the-OECD-metropolitan-database.pdf)
1045 | [the-OECD-metropolitan-database.pdf](http://www.oecd.org/gov/regional-policy/Definition-of-Functional-Urban-Areas-for-the-OECD-metropolitan-database.pdf) (last access: 13 February 2015), 2013.

1046 | Ortega, I. K., Suni, T., Boy, M., Grönholm, T., Manninen, H. E., Nieminen, T., Ehn, M.,
1047 | Junninen, H., Hakola, H., Hellén, H., Valmari, T., Arvela, H., Zegelin, S., Hughes, D.,
1048 | Kitchen, M., Cleugh, H., Worsnop, D. R., Kulmala, M., and Kerminen, V.-M.: New
1049 | insights into nocturnal nucleation, *Atmos. Chem. Phys.*, 12, 4297-4312, 2012.

1050 | [Pierce, J.R., and Adams, P.J.: Efficiency of cloud condensation nuclei formation from](#)
1051 | [ultrafine particles, Atmos. Chem. and Phys., 7, 1367-1379, 2007.](#)

1052 | Pierce, J. R., and Adams, P. J.: Can cosmic rays affect cloud condensation nuclei by
1053 | altering new particle formation rates?, *Geophys. Res. Lett.*, 36, L09820,
1054 | doi:10.1029/2009GL037946, 2009.

1055 | Pikridas, M., [et al Riipinen, I., Hildebrandt, L., Kostenidou, E., Manninen, H. E.,](#)
1056 | [Mihalopoulos, N., Kalivitis, N., Burkhardt, J. F., Stohl, A., Kulmala, M., and Pandis, S.](#)
1057 | [N.:](#) New particle formation at a remote site in the eastern Mediterranean, *J. Geophys.*
1058 | *Res.*, 117, D12205, [doi:10.1029/2012JD017570,](#) [doi:10.1029/2012JD017570,](#) 2012.

1059 | [Platt, S., Haddad, I., Zardini, A., Clairotte, M., Astorga, C., Wolf, R., Slowik, J., Temime-](#)
1060 | [Roussel, B., Marchand, N., Ježek, I., Drinovec, L., Močnik, G., Möhler, O., Richter, R.,](#)
1061 | [Barmet, P., Bianchi, F., Baltensperger, U. and Prévôt, A.:](#) Secondary organic aerosol
1062 | [formation from gasoline vehicle emissions in a new mobile environmental reaction](#)
1063 | [chamber, Atmos. Chem. Phys., 13, 9141–9158, doi:10.5194/acp-13-9141-2013, 2013.](#)

1064 | Pope, C.A., Burnett, R.T., Thun, M.J., Calle, E.E., Krewski, D., Ito, K. and Thurston, G.D.:
1065 | Lung cancer, cardiopulmonary mortality and long term exposure to fine particulate air
1066 | pollution, *J. Am. Med. Assoc.*, 287, 1132-1141, 2002.

1067 | Pope, C. A., Ezzati, M., and Dockery, D. W.: Fine-particulate air pollution and life
1068 | expectancy in the United States, *New Engl. J. Med.* 360, 376–386, 2009.

1069 | [Randerson, J., Chen, Y., Werf, G., Rogers, B. and Morton, D.: Global burned area and](#)
1070 | [biomass burning emissions from small fires, *J. Geophys. Res.*, 117\(G4\),](#)
1071 | [doi:10.1029/2012JG002128, 2012.](#)

1072 | Riccobono, F., Schobesberger, S., Scott, C., Dommen, J., Ortega, I., Rondo, L., Almeida,
1073 | J., Amorim, A., Bianchi, F., Breitenlechner, M., David, A., Downard, A., Dunne, E.,
1074 | Duplissy, J., Ehrhart, S., Flagan, R., Franchin, A., Hansel, A., Junninen, H., Kajos, M.,
1075 | Keskinen, H., Kupc, A., Kurten, A., Kvashin, A., Laaksonen, A., Lehtipalo, K.,
1076 | Makhmutov, V., Mathot, S., Nieminen, T., Onnela, A., Petaja, T., Praplan, A., Santos,
1077 | F., Schallhart, S., Seinfeld, J., Sipila, M., Spracklen, D., Stozhkov, Y., Stratmann, F.,
1078 | Tome, A., Tsagkogeorgas, G., Vaattovaara, P., Viisanen, Y., Vrtala, A., Wagner, P.,
1079 | Weingartner, E., Wex, H., Wimmer, D., Carslaw, K., Curtius, J., Donahue, N., Kirkby,
1080 | J., Kulmala, M., Worsnop, D. and Baltensperger, U.: Oxidation products of biogenic
1081 | emissions contribute to nucleation of atmospheric particles, *Science*, 344, 717-721,
1082 | 2014.

1083 | Rouil, L., Honore, C., Vautard, R., Beekmann, M., Bessagnet, B., Malherbe, L., Meleux,
1084 | F., Dufour, A., Elichegaray, C., Flaud, J-M., Menut, L., Martin, D., Peuch, A., Peuch,
1085 | V-H., Poisson, N.: PREV'AIR : an operational forecasting and mapping system for air
1086 | quality in Europe, *BAMS*, doi: 10.1175/2008BAMS2390.1, 2009.

1087 | Rodríguez, S., Van Dingenen, R., Putaud, J.-P., Roselli, D.: [Nucleation and growth of new](#)
1088 | [particles in the rural atmosphere of Northern Italy—relationship to air quality](#)
1089 | [monitoring. *Atmos. Nucleation and growth of new particles in the rural atmosphere of*](#)
1090 | [Northern Italy relationship to air quality monitoring. *Atmos. Environ.*, 39, 6734-6746,](#)
1091 | 2005.

1092 | Ruuskanen, J., Tuch, T., [h. Ten Brink, T. H. and ..](#), Peters, A., [Khlystov, A., Mirme, A.,](#)
1093 | [Kos, G. P. A., Brunekreef, B., Wichmann, H. E., Buzorius, G., Vallius, M., Kreyling,](#)
1094 | [W. G., and Pekkanen, J.:](#) Concentrations of ultrafine, fine and PM_{2.5} particles in three
1095 | European cities, *Atmos. Environ*, 35, 3729-3738, 2001.

1096 | Sciare, J., d'Argouges, O., Zhang, Q. J., Sarda-Estève, R., Gaimoz, C., Gros, V.,
1097 | Beekmann, M., and Sanchez, O.: Comparison between simulated and observed
1098 | chemical composition of fine aerosols in Paris (France) during springtime: contribution
1099 | of regional versus continental emissions, *Atmos. Chem. Phys.*, 10, 11987–12004, 2010.

1100 | Shi, Q.: Aerosol size distributions (3nm to 3mm) measured at the St. Louis Supersite
1101 | (4/1/01–4/30/02). M.S. Thesis, Department of Mechanical Engineering, University of
1102 | Minnesota, Minneapolis, MN 55455. 2003.

1103 | Shi, Q., Sakurai, H., and McMurry, P. H.: Characteristics of regional nucleation events in
1104 | urban East St. Louis, *Atmos. Environ.*, 41, 4119–4127, 2007.

1105 | [Skylakou, K., Murphy, B. N., Megaritis, A. G., Fountoukis, C., and Pandis, S. N.:](#)
1106 | [Contributions of local and regional sources to fine PM in the megacity of Paris, *Atmos.*](#)
1107 | [Chem. Phys.](#), 14, 2343-2352, doi:10.5194/acp-14-2343-2014, 2014.

1108 | Stanier, C. O., Khlystov, A., and Pandis, S. N.: Nucleation events during the Pittsburgh Air
1109 | Quality Study: Description and relation to key meteorological, gas-phase, and aerosol
1110 | parameters, *Aerosol Sci. Technol*, 38(S1), 253–264, 2004a.

1111 | Stanier C. O., Khlystov, A. Y., and Pandis S. N.: Ambient aerosol size distributions and
1112 | number concentrations measured during the Pittsburgh Air Quality Study, *Atmos.*
1113 | *Environ.*, 38, 3275–3284, 2004b.

1114 | Stohl, A., Forster, V., Frank, A., Seibert, P., and Wotawa, G.: Technical Note: The
1115 | Lagrangian particle dispersion model FLEXPART version 6.2, *Atmos. Chem. Phys.*, 5,
1116 | 2461–2474, 2005.

- 1117 Tuch, T., Wehner, B., Pitz, M., Cyrus, J., Heinrich, J., Kreyling, W. G., Wichmann, H. E.,
 1118 and Wiedensohler, A.: Long-term measurements of size-segregated ambient aerosol in
 1119 two German cities located 100 km apart, *Atmos. Environ.* 37, 4687–4700, 2003.
- 1120 Tuch, T. M., Haudek, A., Müller, T., Nowak, A., Wex, A., and Wiedensohler, A.: Design
 1121 and performance of an automatic regenerating adsorption aerosol dryer for continuous
 1122 operation at monitoring sites, *Atmos. Meas. Tech.*, 2, 417-422, 2009.
- 1123 United Nations, Revision of World Urbanization Prospects, New York, 2014.
- 1124 Vana, M., Kulmala, M., Dal Maso, M., Horrak, U. and Tamm, E.: Comparative study of
 1125 nucleation mode aerosol particles and intermediate air ions formation events at three
 1126 sites, *J. Geophys. Res.* 109, D7201, doi: 10.1029/2003JD004413, 2004.
- 1127 Vana, M., Ehn, M., Petäjä, T., Vuollekoski, H., Aalto, P., de Leeuw, G., Ceburnis, D.,
 1128 O'Dowd, C. D., and Kulmala, M.: Characteristic features of air ions at Mace Head on
 1129 the west coast of Ireland, *Atmos. Res.*, 90, 278, doi:10.1016/j.atmosres.2008.04.007,
 1130 2008.
- 1131 von der Weiden-Reinmüller, S.-L., Drewnick, F., Crippa, M., Prévôt, A. S. H., Meleux, F.,
 1132 Baltensperger, U., Beekmann, M., and Borrmann, S.: Application of mobile aerosol and
 1133 trace gas measurements for the investigation of megacity air pollution emissions: the
 1134 Paris metropolitan area, *Atmos. Meas. Tech.*, 7, 279-299, 2014a.
- 1135 von der Weiden-Reinmüller, S.-L., Drewnick, F., Zhang, Q. J., Freutel, F., Beekmann, M.,
 1136 and Borrmann, S.: Megacity emission plume characteristics in summer and winter
 1137 investigated by mobile aerosol and trace gas measurements: the Paris metropolitan area,
 1138 *Atmos. Chem. Phys.*, 14, 11931-11250, 2014b.
- 1139 [Wählin, P., Palmgren, F., Dingenen, R. and Raes, F.: Pronounced decrease of ambient](#)
 1140 [particle number emissions from diesel traffic in Denmark after reduction of the sulphur](#)
 1141 [content in diesel fuel, *Atmos. Environ.*, 35, 35493552, doi:10.1016/S1352-](#)
 1142 [2310\(01\)00066-8, 2001.](#)
- 1143 Wählin, Peter.: Measured reduction of kerbside ultrafine particle number concentrations in
 1144 Copenhagen, *Atmos. Environ.*, 43, 3645–3647, 2009.
- 1145 Wang, Z., Hopke, P. K., Ahmadi, G., Cheng, Y. S., and Baron, P. A.: Fibrous particle
 1146 deposition in human nasal passage: The influence of particle length, flow rate, and
 1147 geometry of nasal airway, *J. Aerosol Sci.*, 39, 1040–1054, 2008.
- 1148 Wang, F., Costabile, F., Li, H., Fang, D., Alligrini, I.: Measurements of ultrafine particle
 1149 size distribution near Rome, *Atmos. Res.* 98, 69–77, 2010.
- 1150 Watson, J. G., Chow, J. C., Lowenthal, D. H., Kreisberg, N. M., Hering, S. V., and
 1151 Stolzenburg, M. R.: Variations of nanoparticle concentrations at the Fresno Supersite,
 1152 *Sci. Tot. Environ.*, 358, 178–187, 2006.
- 1153 Wehner, B. and Wiedensohler, A.: Long term measurements of submicrometer urban
 1154 aerosols: statistical analysis for correlations with meteorological conditions and trace
 1155 gases, *Atmos. Chem. Phys.* 3, 867-879, 2003.
- 1156 Wehner, B., Wiedensohler, A., [Tuch, T. T.M.](#), Wu, Z. J., Hu, M., Slanina, J., and Kiang, C.
 1157 S.: Variability of the aerosol number size distribution in Beijing, China: new particle
 1158 formation, dust storms, and high continental background, *Geophys. Res. Lett.*, 31,
 1159 L22108, [doi:10.1029/2004GL021596](#) 2004.
- 1160 Wehner, B., Siebert, H., Stratmann, F., Tuch, T., Wiedensohler, A., Petäjä, T., Dal Maso,
 1161 M. and Kulmala, M.: Horizontal homogeneity and vertical extent of new particle
 1162 formation events, *Tellus, B*, 59(3), 362–371, doi:10.1111/j.1600-0889.2007.00260.x,
 1163 2007.
- 1164 Weimer, S., C. Mohr, R. Richter, J. Keller, M. Mohr, A. S. H. Prévôt, and U.
 1165 Baltensperger.: Mobile measurements of aerosol number and volume size distributions

1166 in an Alpine valley: Influence of traffic versus wood burning, *Atmos. Environ.*, 43, 624-
1167 630, 2009.

1168 Wen, J., Zhao, Y., and Wexler, A. S.: Marine particle nucleation: Observation at Bodega
1169 Bay, California, *J. Geophys. Res.*, 111, D08207, doi:10.1029/2005JD006210, 2006.

1170 Woo, K. S., Chen, D. R., Pui, D. Y. H. and McMurry, P. H.: Measurement of Atlanta
1171 aerosol size distributions: Observations of ultrafine particle events, *Aerosol Sci.*
1172 *Technol.*, 34, 75-87, 2001.

1173 [World Bank: World Development Report 2012: World Development Indicators, Fossil](#)
1174 [Fuel Energy Consumption, 2012.](#)

1175 Wu, Z.J., Hu, M., Liu, S., Wehner, B., Bauer, S., Maßling, A., Wiedensohler, A., Petaja ,
1176 T., Dal Maso, M., Kulmala, M.: New particle formation in Beijing, China: statistical
1177 analysis of a 1-year data set. *J. Geophys. Res.*, 112, D09209.
1178 doi:10.1029/2006JD007406, 2007.

1179
1180
1181
1182
1183
1184
1185
1186

1187 [Zhang, Q. J., Beekmann, M., Drewnick, F., Freutel, F., Schneider, J., Crippa, M.,](#)
1188 [Prevot, A. S. H., Baltensperger, U., Poulain, L., Wiedensohler, A., Sciare, J., Gros, V.,](#)
1189 [Borbon, A., Colomb, A., Michoud, V., Doussin, J.-F., Denier van der Gon, H. A. C.,](#)
1190 [Haefelin, M., Dupont, J.-C., Siour, G., Petetin, H., Bessagnet, B., Pandis, S. N.,](#)
1191 [Hodzic, A., Sanchez, O., Honoré, C., and Perrussel, O.: Formation of organic aerosol in](#)
1192 [the Paris region during the MEGAPOLI summer campaign: evaluation of the volatility-](#)
1193 [basis-set approach within the CHIMERE model, *Atmos. Chem. Phys.*, 13, 5767-5790,](#)
1194 [doi:10.5194/acp-13-5767-2013, 2013.](#)

1195 [Zhou, L., Kim, E., Hopke, P., Stanier, C. and Pandis, S.: Advanced Factor Analysis on](#)
1196 [Pittsburgh Particle Size-Distribution Data, *Aerosol Sci. and Technol.*, 38 \(Sup.1\), 118-](#)
1197 [132, doi:10.1080/02786820390229589, 2004.](#)

1198
1199
1200
1201
1202
1203
1204
1205
1206
1207
1208
1209
1210

1211
1212
1213
1214
1215

Table 1. Summary of main MEGAPOLI measurements used in this study.

<u>Variable</u>	<u>Instrument</u>	<u>Group</u>	<u>Time Resoluti</u>	<u>Sample Condition</u>
<u>ATR-42</u>				
<u>Absorption (summer)</u>	<u>PSAP^a</u>	<u>LaMPⁱ</u>	<u>1 sec</u>	<u>dry</u>
<u>Trace Gas Concentration</u>	<u>HS PTR-QMS^b</u>	<u>CNRS^k</u>	<u>1 sec</u>	<u>dry</u>
<u>Aerosol Number Concentration</u>	<u>TSI 3025 CPC^c</u>	<u>CNR^l</u>	<u>1 sec</u>	<u>dry</u>
<u>Aerosol Number Concentration</u>	<u>TSI 3010 CPC^c</u>	<u>LaMPⁱ</u>	<u>1 sec</u>	<u>dry</u>
<u>Absorption (winter)</u>	<u>PSAP^a</u>	<u>CNR^l</u>	<u>1 sec</u>	<u>dry</u>
<u>MoLa</u>				
<u>Aerosol Number Concentration</u>	<u>TSI 3786 UWPCP^d</u>	<u>MPIC_m</u>	<u>1 sec</u>	<u>ambient</u>
<u>MOSQUITA</u>				
<u>Aerosol Number Concentration</u>	<u>TSI 3010 CPC^c</u>	<u>PSIⁿ</u>	<u>1sec</u>	<u>ambient</u>
<u>Aerosol Number Concentration</u>	<u>UHSAS^e</u>	<u>PSIⁿ</u>	<u>1 sec</u>	<u>ambient</u>
<u>SIRTA</u>				
<u>Aerosol Number Size Distribution (10–500 nm)</u>	<u>SMPS^f</u>	<u>UoHP^p</u>	<u>10 min</u>	
<u>Aerosol Number Size Distribution (10–500 nm)</u>	<u>DMPS^g</u>	<u>UoHP^p</u>	<u>9 min</u>	
<u>Positive/Negative Ion Size Distribution (0.8–40 nm)</u>	<u>AIS^h</u>	<u>UoHP^p</u>	<u>3 min</u>	
<u>LHVP</u>				
<u>Aerosol Number Size Distribution (3–200 nm)</u>	<u>DMPS^g</u>	<u>IfT^q</u>	<u>10 min</u>	
<u>GOLF</u>				
<u>Aerosol Number Size Distribution (5–1000 nm)</u>	<u>EASⁱ</u>	<u>MPIC_m</u>	<u>1 min</u>	
<u>Variable</u>	<u>Instrument</u>	<u>Group</u>	<u>Time Resoluti</u>	<u>Sample Condition</u>
<u>ATR-42</u>				
<u>Absorption (summer)</u>	<u>PSAP^a</u>	<u>LaMPⁱ</u>	<u>1 sec</u>	<u>dry</u>
<u>Trace Gas Concentration</u>	<u>HS PTR-QMS^b</u>	<u>CNRS^k</u>	<u>1 sec</u>	<u>dry</u>
<u>Aerosol Number Concentration</u>	<u>TSI 3025 CPC^c</u>	<u>CNR^l</u>	<u>1 sec</u>	<u>dry</u>
<u>Aerosol Number Concentration</u>	<u>TSI 3010 CPC^c</u>	<u>LaMPⁱ</u>	<u>1 sec</u>	<u>dry</u>
<u>Absorption (winter)</u>	<u>PSAP^a</u>	<u>CNR^l</u>	<u>1 sec</u>	<u>dry</u>
<u>MoLa</u>				
<u>Aerosol Number Concentration</u>	<u>TSI 3786 UWPCP^d</u>	<u>MPIC_m</u>	<u>1 sec</u>	<u>ambient</u>
<u>MOSQUITA</u>				
<u>Aerosol Number Concentration</u>	<u>TSI 3010 CPC^c</u>	<u>PSIⁿ</u>	<u>1sec</u>	<u>ambient</u>

<u>Aerosol Number Concentration</u>	<u>UHSAS^c</u>	<u>PSIⁿ</u>	<u>1 sec</u>	<u>ambient</u>
<u>SIRTA</u>				
<u>Aerosol Number Size Distribution</u>	<u>SMPS^f</u>		<u>10 min</u>	<u>dry</u>
<u>Aerosol Number Size Distribution (6– 0.8–40 nm)</u>	<u>DMPS^g</u>	<u>UoH^p</u>	<u>9 min</u>	<u>ambient</u>
<u>LHVP</u>				
<u>Aerosol Number Size Distribution (3– 0.8–40 nm)</u>	<u>DMPS^g</u>	<u>IfT^q</u>	<u>10 min</u>	<u>dry</u>
<u>Positive/Negative Ion Size Distribution (0.8–40 nm)</u>	<u>AIS^h</u>	<u>UoH^p</u>	<u>3 min</u>	<u>ambient</u>
<u>GOLF</u>				
<u>Aerosol Number Size Distribution (5 0.8–40 nm)</u>	<u>EASⁱ</u>	<u>MPIC^m</u>	<u>1 min</u>	<u>ambient</u>

1216

1217 ^aPSAP: Particle Soot Absorption Photometer; ^bHS PTR-QMS: High Sensitivity Proton Transfer
 1218 Reaction-Quadrupole Mass Spectrometer; ^cCPC: Condensation Particle Counter; ^dUWCPC:
 1219 Ultrafine Water Condensation Particle Counter; ^eUHSAS: Ultra High Sensitivity Aerosol
 1220 Spectrometer; ^fSMPS: Scanning Mobility Particle Sizer; ^gDMPS: Differential Mobility Particle
 1221 Sizer; ^hAIS: Air Ion Spectrometer; ⁱEAS: Electrical Aerosol Spectrometer; ^jLaMP: Laboratoire
 1222 Meteorologie Physique; ^kCNRS: Centre national de la recherche scientifique; ^lCNRM: Centre
 1223 National de Recherches Météorologiques; ^mMPIC: Max Planck Institute for Chemistry; ⁿPSI: Paul
 1224 Scherrer Institute; ^oCMU: Carnegie Mellon University; ^pUoH: University of Helsinki; ^qIfT: Leibniz
 1225 Institute for Tropospheric Research.

1226

1227 **Table 2.** Aerosol number concentrations during the summer and winter campaigns and
1228 characteristics of NPF during summer. σ is the standard deviation.

1229

<i>Site</i>	Average $\pm 1\sigma$ Number Concentration (10 - 500 nm) 1000/cm³		Average increase$\pm 1\sigma$ in Number Concentration due to NPF (%)	Growth Rate $\pm 1\sigma$ (nm h⁻¹)
	<i>Summer</i>	<i>Winter</i>	<i>Summer</i>	<i>Summer</i>
GOLF	13.3 \pm 6.8	25.3 \pm 15.1	127 \pm 110	6.1 \pm 1.8
LHVP	11.4 \pm 5.1	15.6 \pm 7.1	100 \pm 50	4.6 \pm 1.9
SIRTA	5.3 \pm 3.1	10.1 \pm 5.7	129 \pm 59	5.5 \pm 4.1

1230

1231

1232

1233

1234

1235

1236

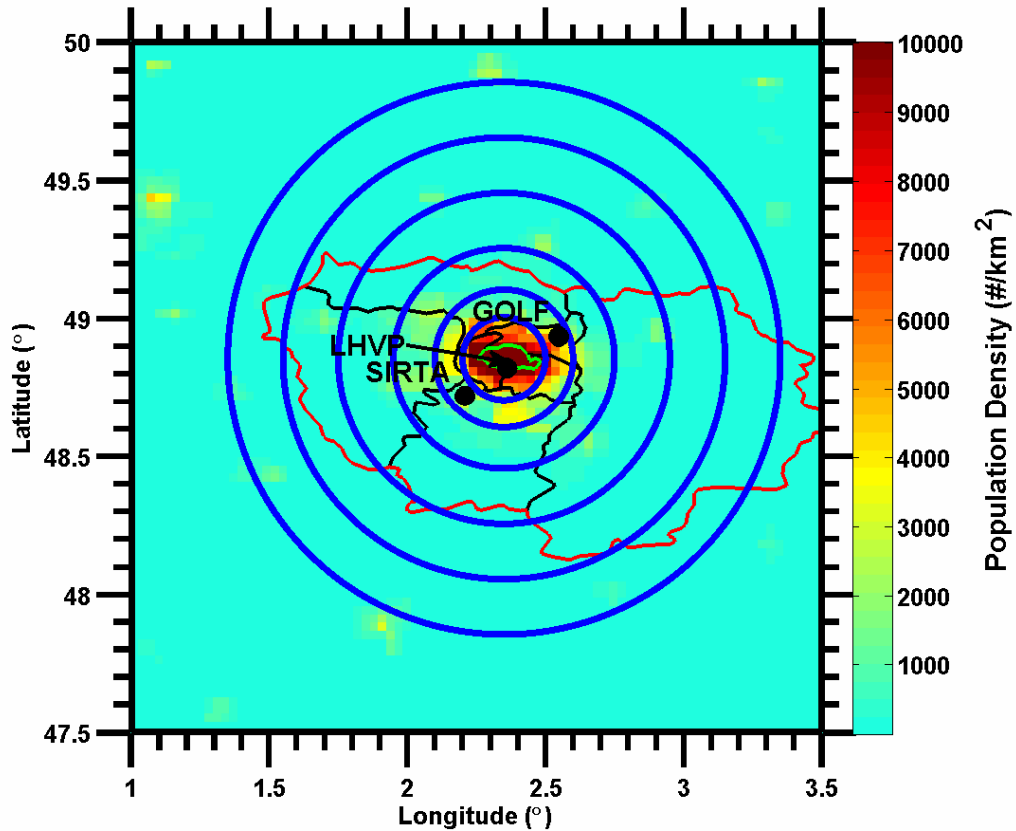
1237

1238

1239

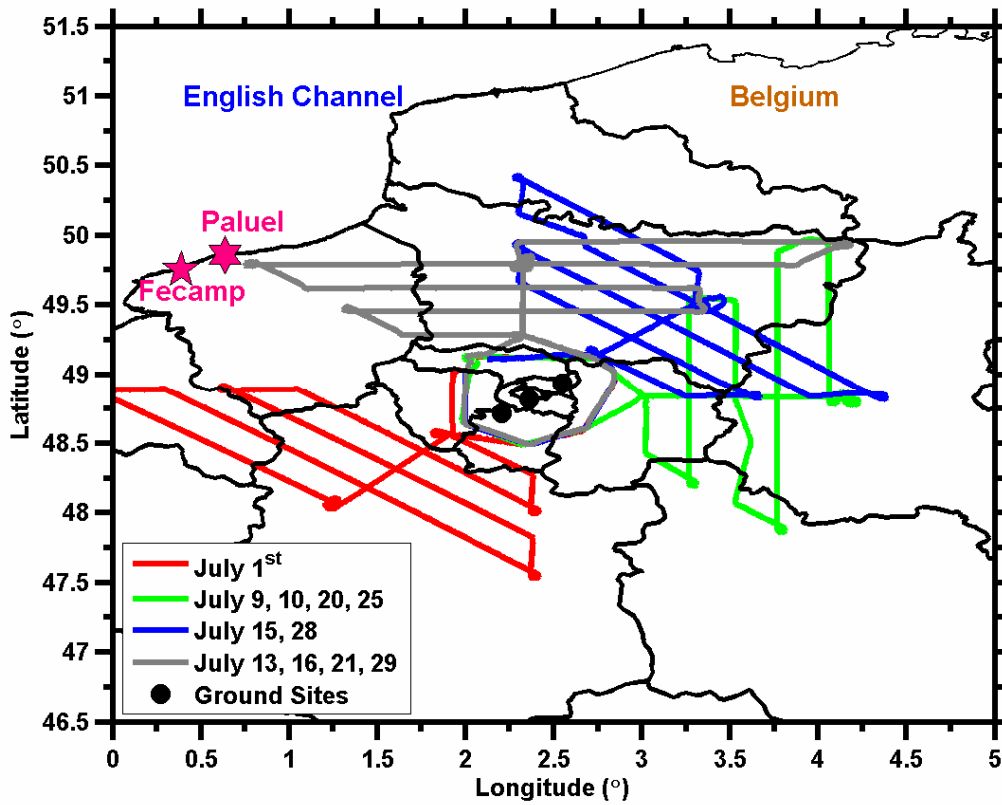
1240

1241



1242
 1243
 1244
 1245
 1246
 1247
 1248
 1249
 1250
 1251
 1252
 1253
 1254
 1255
 1256
 1257
 1258
 1259
 1260
 1261
 1262
 1263
 1264
 1265

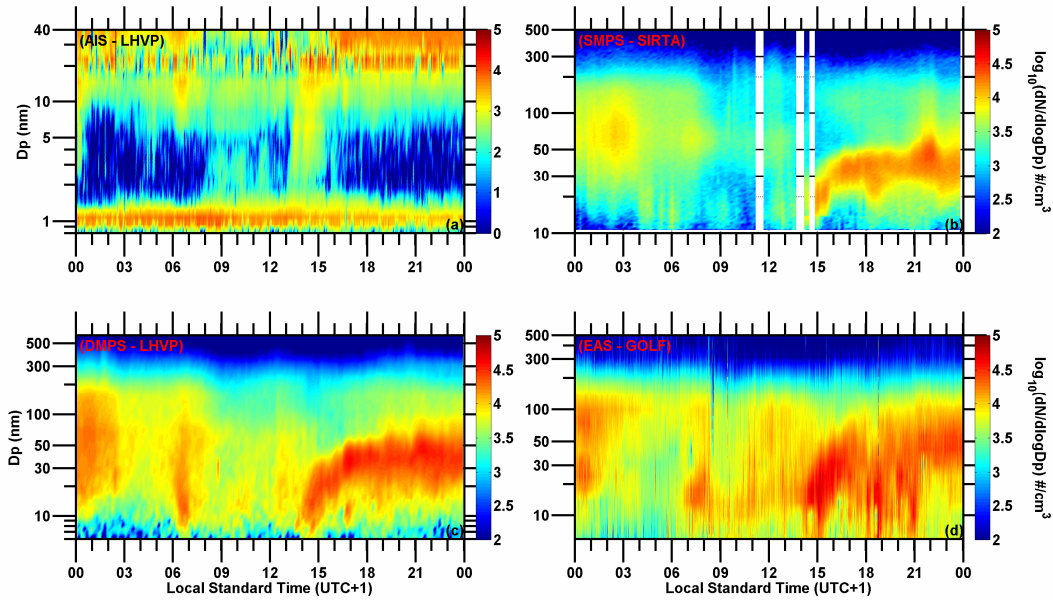
Fig. 1. Population density and administrative map of Paris. Outlined in red is Île de France and in green Paris. The three ground stations (SIRTA, LHVP and GOLF) are depicted with black dots. The map is separated into sectors depicted by blue lines, formed by concentric circles centered at kilometer zero of Paris (48.8534 °N 2.3488 °E). The radius of the circles is 0.15, 0.25, 0.4, 0.6, 0.8 and 1 °, which corresponds to 16.7, 27.8, 44.4, 66.7, 88.9 and 111.1 km.



1266
 1267
 1268
 1269
 1270
 1271
 1272
 1273
 1274
 1275
 1276
 1277
 1278
 1279
 1280
 1281
 1282
 1283
 1284
 1285
 1286
 1287
 1288
 1289
 1290
 1291
 1292
 1293
 1294
 1295

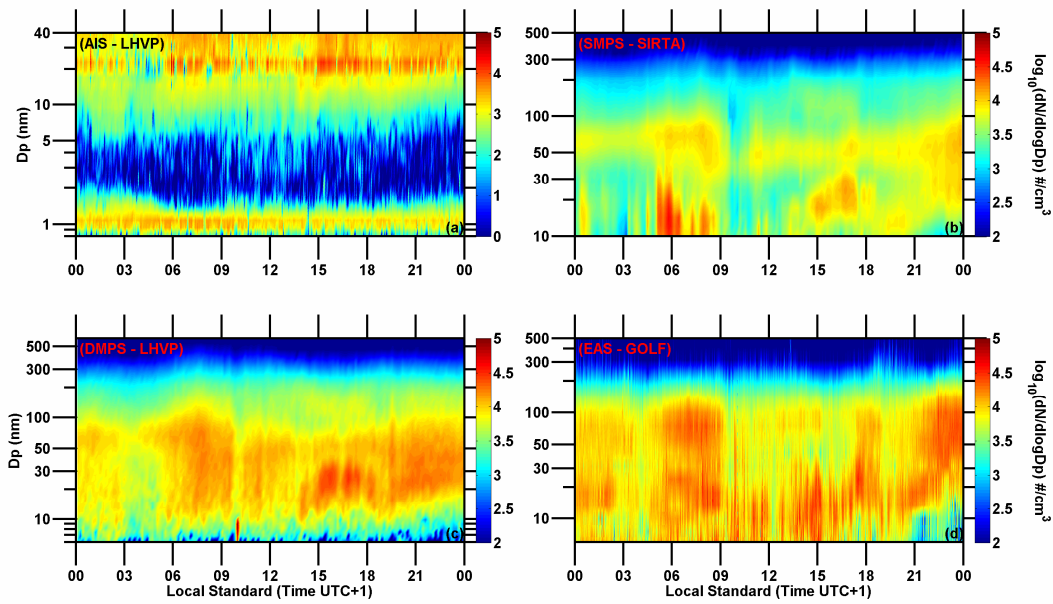
Fig. 2. Flight paths of the ATR-42 aircraft during the summer campaign. Different colors correspond to different flight routes. The cities of Fecamp and Paluel are also depicted in the map.

1296
1297
1298
1299
1300



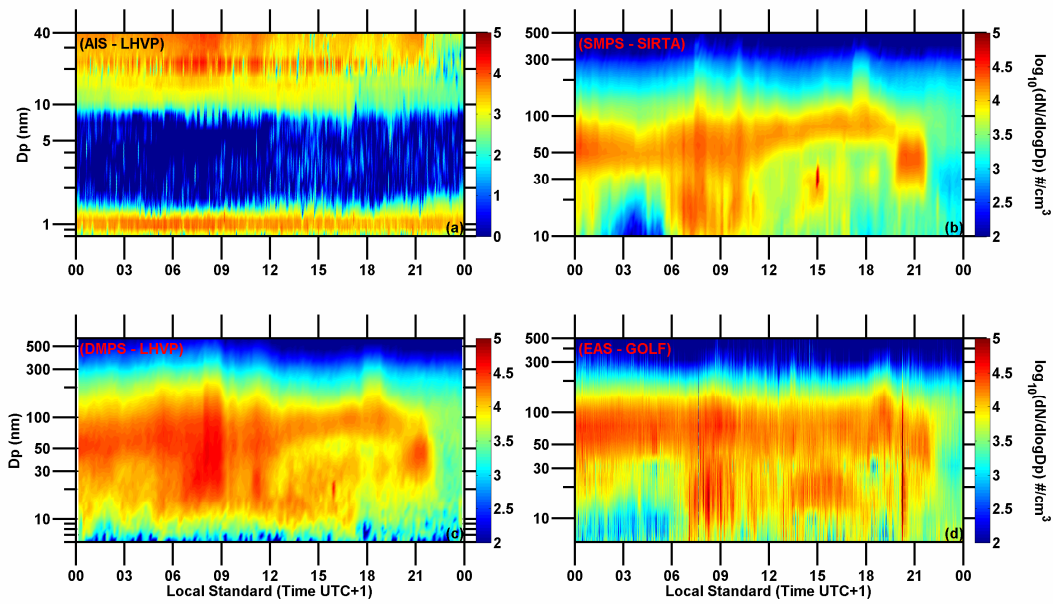
1301
1302
1303
1304
1305
1306
1307
1308
1309
1310
1311
1312
1313
1314
1315

Fig. 3. Size distribution measurements during a nucleation event day (12 July 2009) at all ground sites. (a) AIS measurements at [SIRTALHVP](#), (b) SMPS measurements at [SIRTA](#), (c) DMPS measurements at [LHVP](#), (d) EAS measurements at [GOLF](#). Time of day corresponds to local standard time (UTC+1). D_p is the particle diameter.



1316
 1317
 1318
 1319
 1320
 1321
 1322
 1323
 1324
 1325
 1326
 1327
 1328
 1329
 1330
 1331
 1332
 1333
 1334

Fig. 4. Size distribution measurements during an undefined event day (10 July 2009): (a) AIS measurements at [SIRTALHVP](#), (b) SMPS measurements at SIRTA, (c) DMPS measurements at LHVP, (d) EAS measurements at GOLF. Time of day corresponds to local standard time (UTC+1). D_p is the particle diameter.

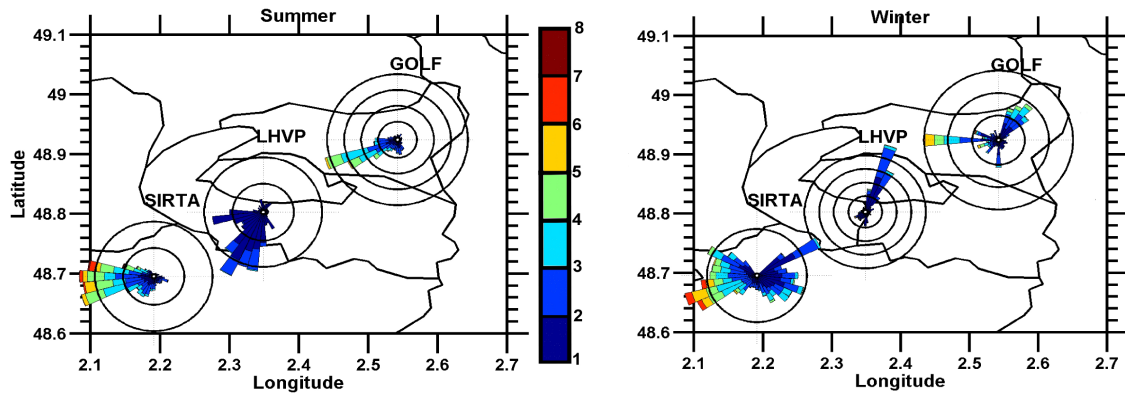


1335
 1336
 1337
 1338
 1339
 1340
 1341
 1342
 1343
 1344
 1345
 1346
 1347
 1348
 1349
 1350
 1351
 1352
 1353
 1354
 1355
 1356
 1357

Fig. 5. Size distribution measurements during a non-event day (29 July 2009): (a) AIS measurements at [SIRTALHVP](#), (b) SMPS measurements at SIRT, (c) DMPS measurements at LHVP, (d) EAS measurements at GOLF. Time of day corresponds to local standard time (UTC+1). D_p is the particle diameter.

1358

1359



1360

1361

1362

1363

1364

1365

1366

1367

Fig. 6. Wind direction rose plots during the summer and winter campaigns at each of the ground sites. Each rose segment corresponds to an angle bin of $\pi/18$ (i.e. 20°) and concentric circles at each site correspond to 5% relative frequency. Wind speed, in m s^{-1} , corresponding to each size bin is color coded inside each rose. Wind speeds below 1 m s^{-1} have been omitted from the graph.

1368

1369

1370

1371

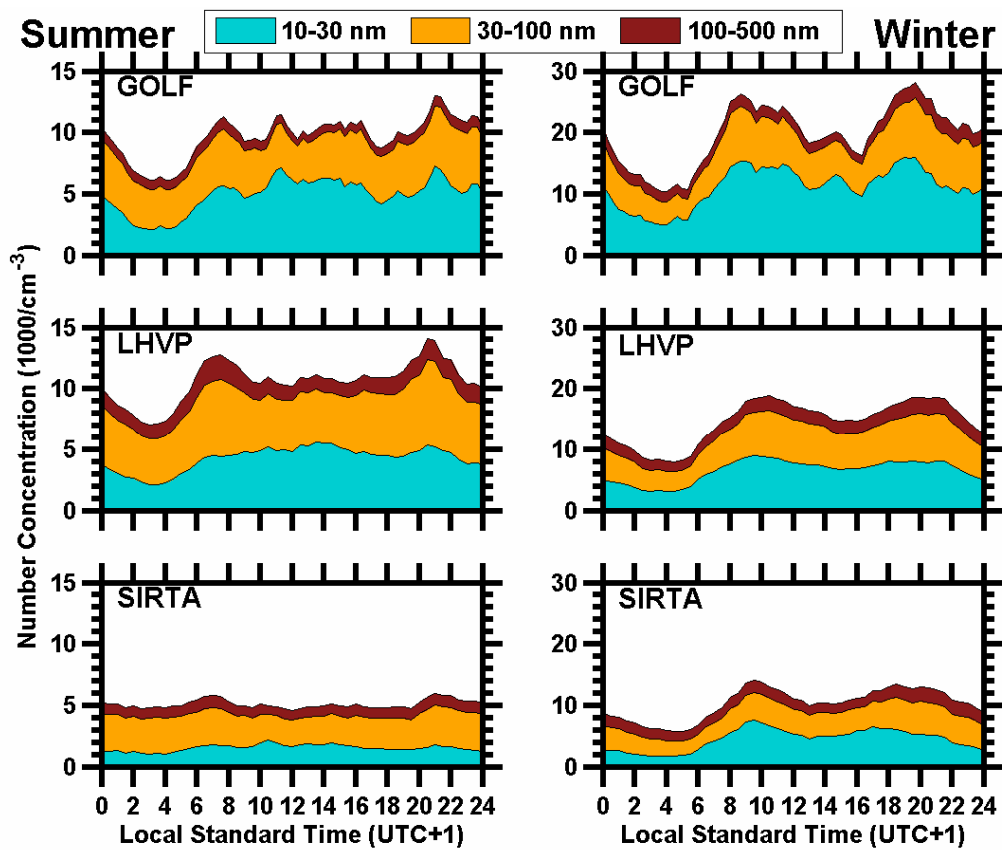
1372

1373

1374

1375

1376



1377

1378

1379

1380 **Fig. 7.** Number concentration diurnal profiles of summer (left) and winter (right)
 1381 campaigns for size ranges from 10 to 30 nm, 30 to 100 nm, and 100 to 500 nm,
 1382 respectively. Different scales are used for each season.

1383

1384

1385

1386

1387

1388

1389

1390

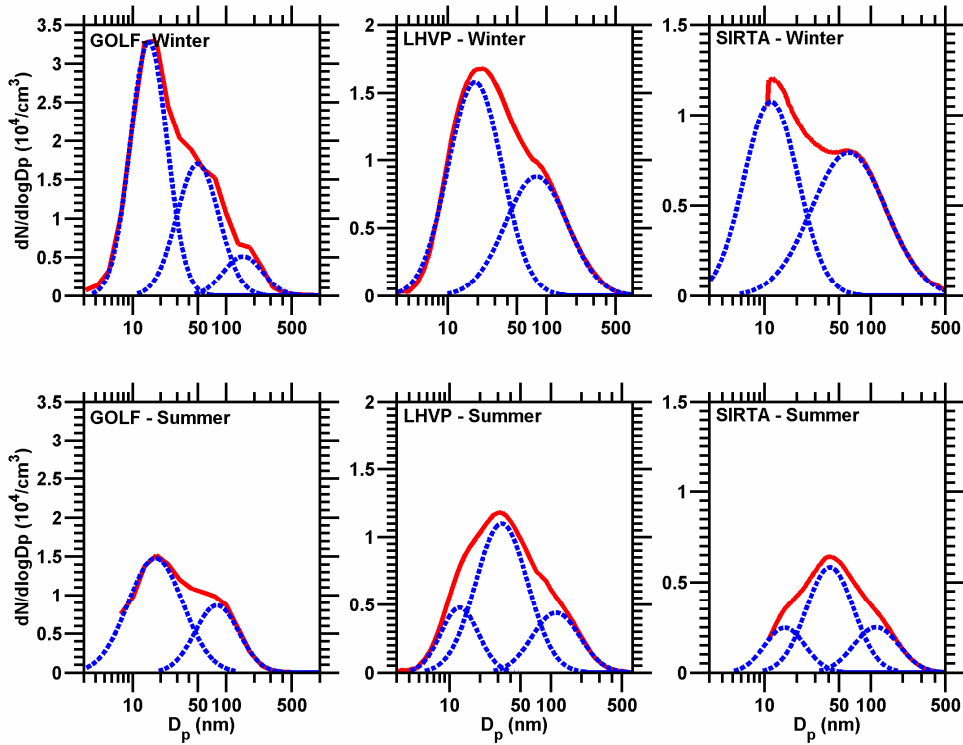
1391

1392

1393

1394

1395
1396
1397



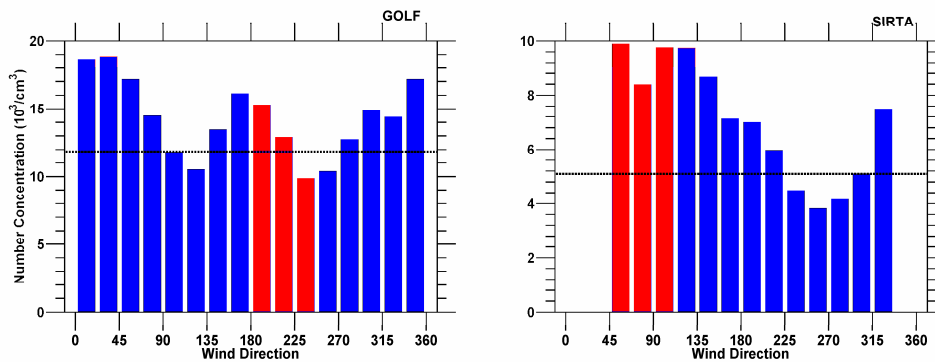
1398
1399
1400
1401
1402
1403
1404
1405

1406
1407
1408
1409
1410
1411
1412
1413
1414
1415

Fig. 8. Campaign average particle number size distributions for winter (top) and summer (red) and winter (black) of all bottom for the three ground sites based on measurements of EAS at GOLF, DMPS at LHVP and SMPS at SIRTA. Each average size distribution (solid red line) is deconvoluted to lognormal modes (dashed blue lines). Note the different scaling of the y-axes. between sites.

1416

1417



1418

1419

1420

1421

1422

1423

1424

1425

1426

Fig. 9. Number concentrations measured at the two satellite sites during summer with respect to wind direction / air mass transport direction measured at the respective site. The angles which indicate that the air mass traveled through the city center prior to reaching the site are depicted in red. The horizontal dashed black line corresponds to the campaign average for each site. Periods with wind speed below 1 m s⁻¹ were omitted from the analysis.

1427

1428

1429

1430

1431

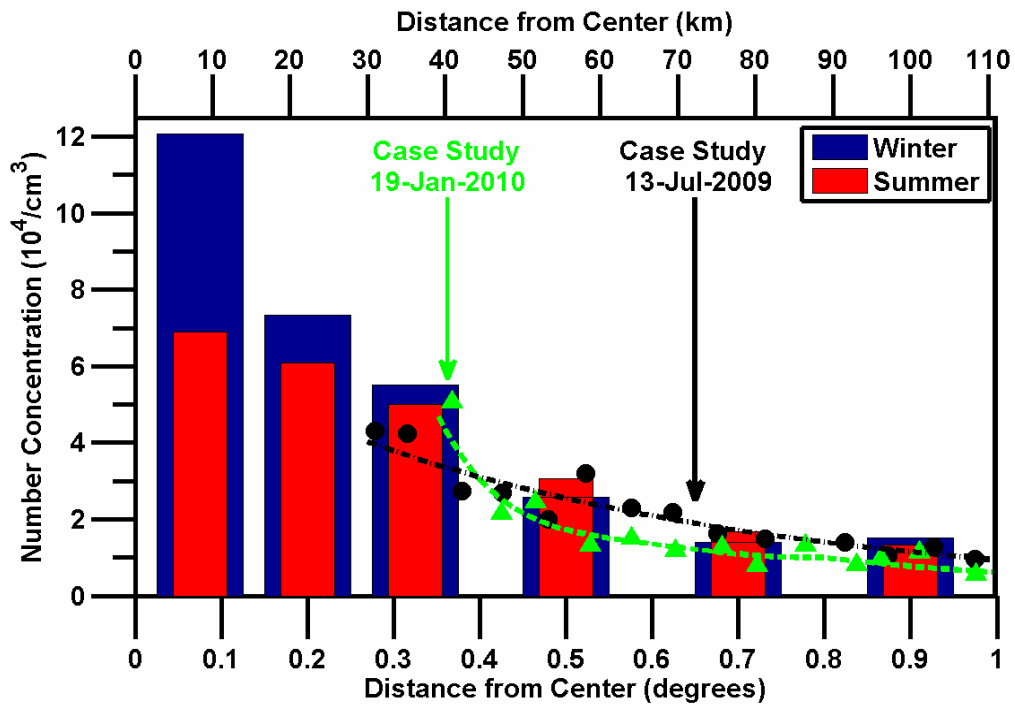
1432

1433

1434

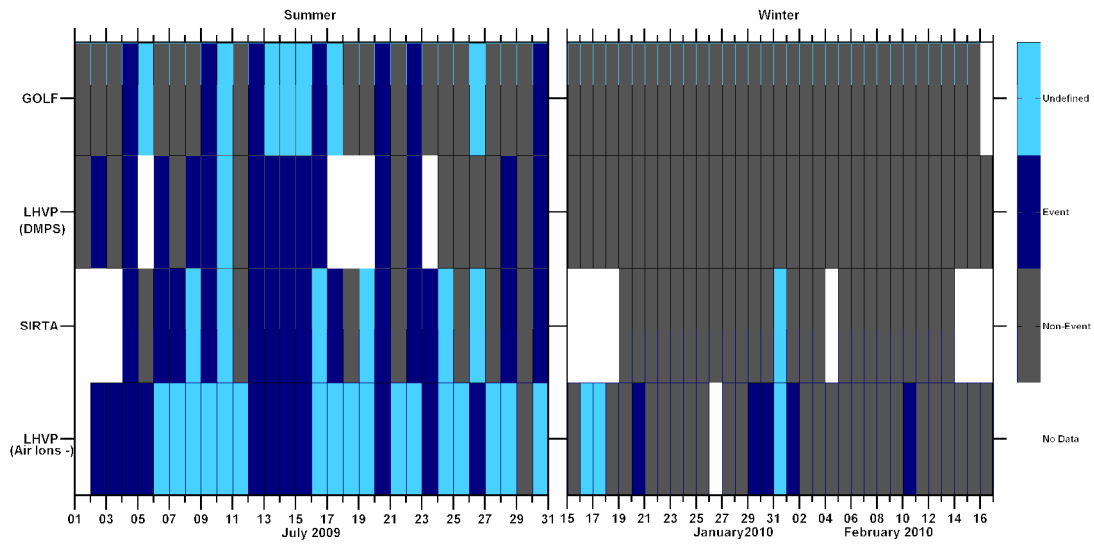
1435

1436



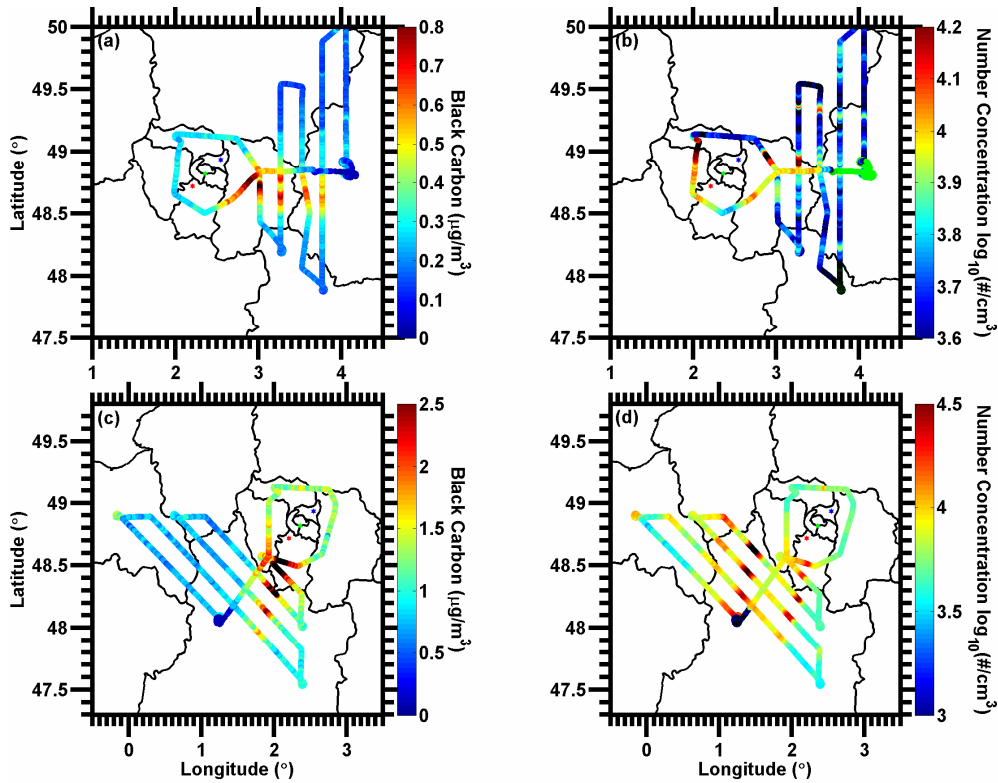
1437
 1438
 1439
 1440
 1441
 1442
 1443
 1444
 1445
 1446
 1447
 1448
 1449
 1450
 1451
 1452
 1453
 1454
 1455
 1456
 1457

Fig. 10. Average number concentration ($N_{2.5}$) with respect to distance from the city center measured by the mobile platforms during summer (red) and winter (blue). During both campaigns an exponential decrease of the number concentration with respect to distance was observed. The number concentration measured in an axial measurement on a case study day is also depicted in the graph for summer (black dots) and winter (green triangles).



1458
 1459
 1460
 1461
 1462
 1463
 1464
 1465
 1466
 1467
 1468
 1469
 1470
 1471
 1472
 1473
 1474
 1475
 1476
 1477
 1478
 1479
 1480
 1481
 1482
 1483
 1484

Fig. 11. Nucleation analysis results during summer and winter for all ground sites. Events, non-events, undefined and lack of data are depicted in blue, grey, light blue and white, respectively.



1485

1486

1487 **Fig. 12.** Flight trajectories for 9th (a, b) and 1st (c, d) July 2009, color coded for black
 1488 carbon and number concentrations (N_{10}), respectively. Black carbon concentrations are
 1489 used as tracers of the Paris plume (a, c); its direction relative to the city center indicates
 1490 wind direction. Red, green and black dots within the figure correspond to the locations
 1491 of SIRTA, LHVP and GOLF, respectively. Increased number concentrations were
 1492 observed outside of the plume. During July 9 (b) the area where the number
 1493 concentration increased was located upwind of the city center and NPF was identified at
 1494 all ground sites. During July 1 (d) the particle number increase was observed along the
 1495 plume. The number and black carbon concentration corresponding to c and d are also
 1496 shown with respect to time in Suppl. Fig. 3.

1497

1498

1499

1500

1501

1502

1503

1504

1505

1506

1507

1508

1509

1510

1511

1512

1513

1514

1515
1516
1517
1518
1519
1520
1521
1522
1523
1524
1525
1526
1527

1528
1529
1530
1531
1532
1533
1534
1535
1536
1537
1538
1539
1540
1541
1542
1543
1544
1545
1546
1547
1548
1549
1550
1551
1552

Supplementary material to

Ultrafine particle sources and in-situ formation in a European Megacity

Michael Pikridas^{1, 2}, Jean Sciare³, Alfons Schwarzenboeck³, Suzanne Crumeyrolle³, Agnes Borbon⁴, Friederike Freutel⁵, Maik Merkel⁶, Sarah-Lena von der Weiden-Reinmüller⁵, Monica Crippa⁷, Evangelia Kostenidou^{1, 2}, Magda Psychoudaki^{1, 2}, Lea Hildebrandt⁸, Gabriella J. Engelhart⁸, Frank Drewnick⁵, Matthias Beekmann⁴, Tuukka Petäjä⁹, Andre S. H. Prevot⁷, Urs Baltensperger⁷, Alfred Wiedensohler⁶, Markku Kulmala⁹, and Spyros N. Pandis^{1,2,8}

¹Department of Chemical Engineering, University of Patras, Greece

²Institute of Chemical Engineering Sciences (ICE), FORTH, Patras, Greece

³Laboratoire Meteorologie Physique (LaMP), 24 avenue des Landais, 63177, Aubiere, France

⁴Laboratoire Interuniversitaire des Systemes Atmospheriques, CNRS, Universites Paris-Est & Paris Diderot, 61 av. Du Gal de Gaulle, 94010 Creteil, France

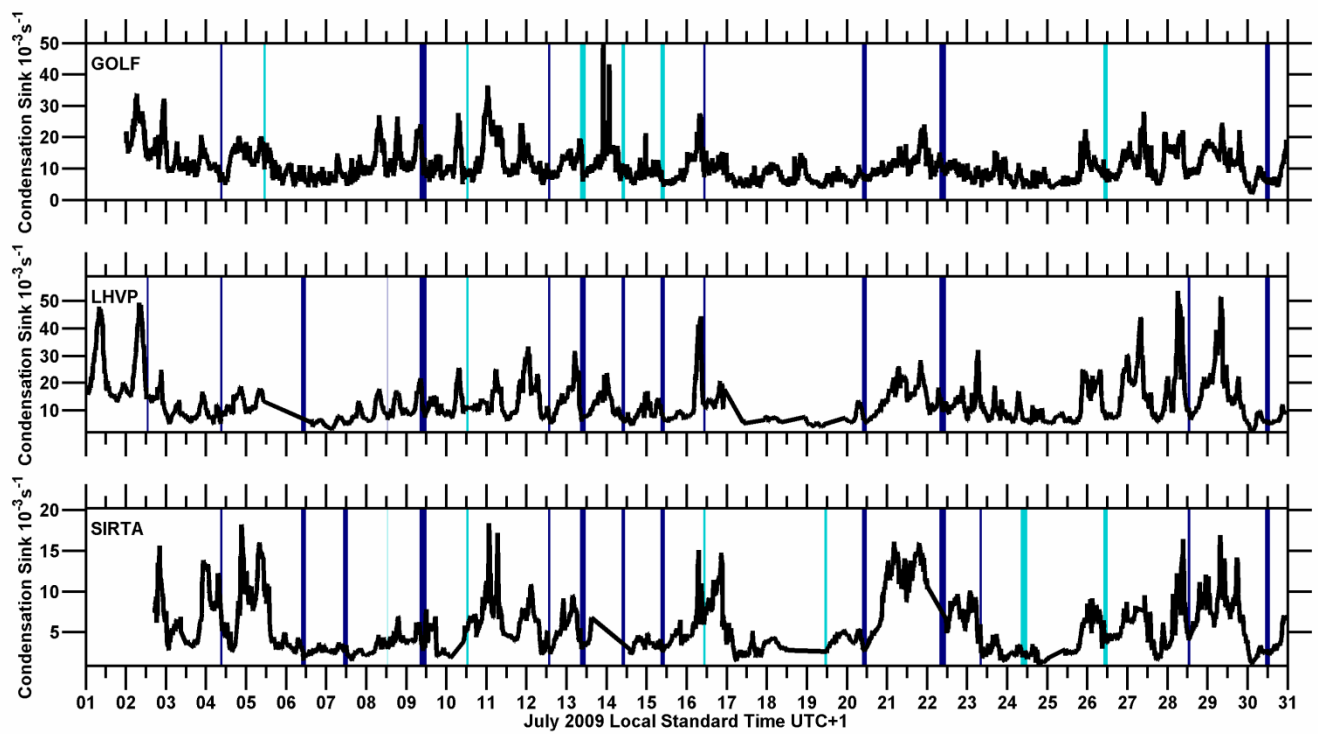
⁵Max Planck Institute for Chemistry, Particle Chemistry Department, Mainz, Germany

⁶Leibniz Institute for Tropospheric Research, Leipzig, Germany

⁷Paul Scherrer Institute, Laboratory of Atmospheric Chemistry, Villigen, Switzerland

⁸Department of Chemical Engineering, Carnegie Mellon University, Pittsburgh, USA

⁹Department of Physics, University of Helsinki, Helsinki, Finland

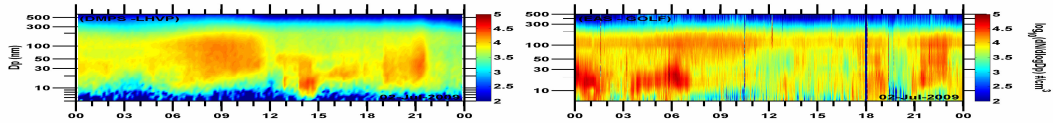


1553 Suppl. Fig.1. Condensation sink measured at the three ground sites during July 2009.

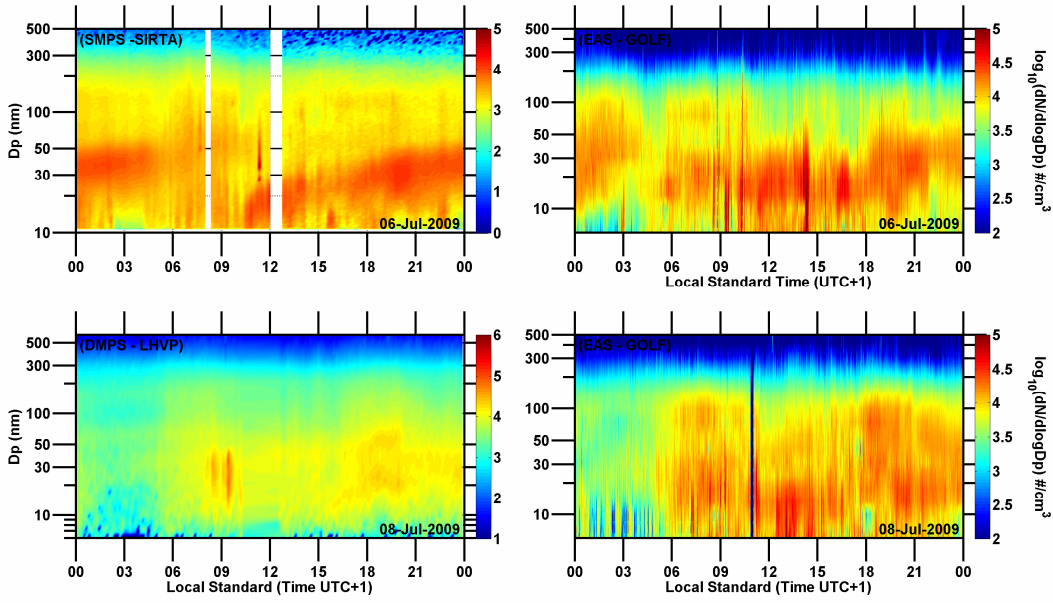
1554 Dark and light blue bars indicate the event and undefined periods, respectively.

- 1555
- 1556
- 1557
- 1558
- 1559
- 1560
- 1561
- 1562
- 1563
- 1564
- 1565
- 1566
- 1567
- 1568
- 1569
- 1570
- 1571
- 1572
- 1573
- 1574
- 1575
- 1576
- 1577
- 1578
- 1579
- 1580
- 1581
- 1582

1583



1584



1585

1586

1587

1588

1589

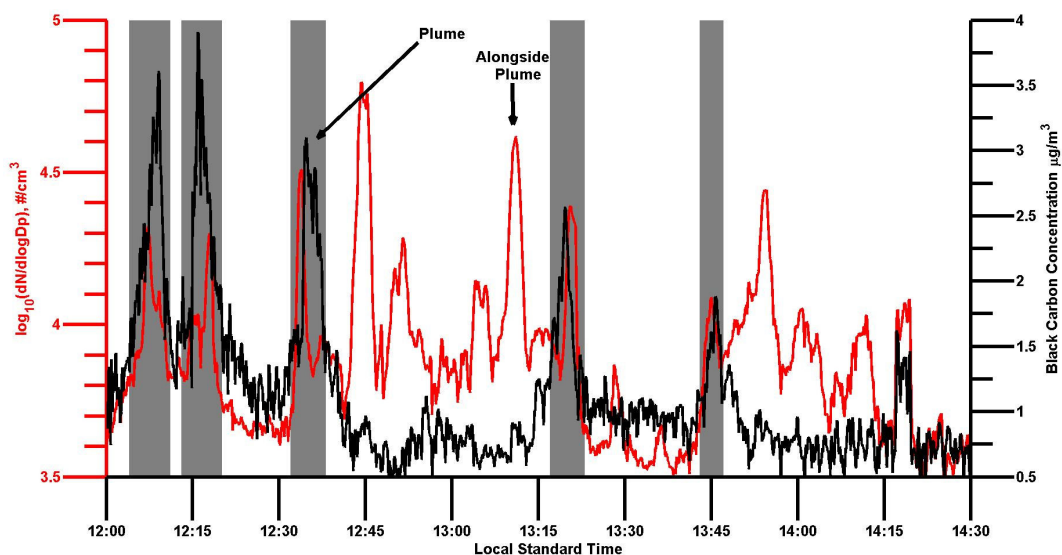
1590

1591

1592

1593

Suppl. Fig. 2. Number size distribution time series when a nucleation event was identified at SIRTA and/or LHVP but not at GOLF. D_p is the particle diameter.

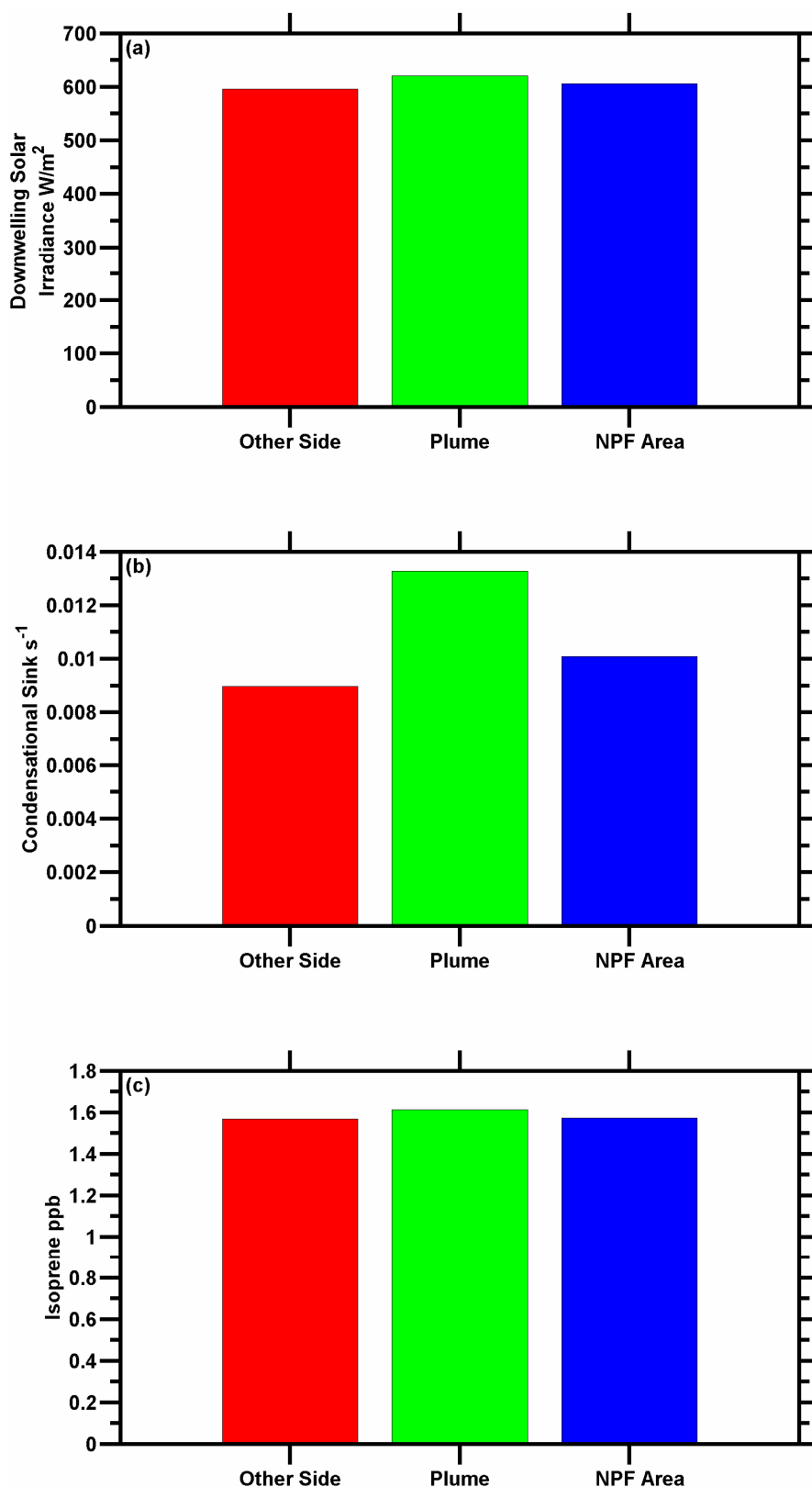


1594

1595 Suppl. Fig. 3. Number (red line) and black carbon (black line) concentrations during
 1596 airborne measurements on July 1st 2009. Number concentration increases observed
 1597 simultaneously with increases in black carbon mass concentration (grey areas) were
 1598 attributed to the Paris plume. Number concentration increases were also observed
 1599 alongside the plume.

1600

1601



1602
 1603
 1604
 1605
 1606
 1607
 1608

Suppl. Fig. 4. Downwelling solar irradiance (top), condensation sink (middle) and isoprene concentration (bottom) comparison of the Paris plume with areas on either side of the plume when high particle concentrations were observed at one side outside of the plume. Significant differences among these areas were not observed with respect to condensation sink, isoprene and solar irradiance.